BMC Plant Biology

RESEARCH

Open Access

Predicting the impact of climate change on the habitat suitability and phytochemical quality of *Salvia multicaulis* Vahl

Mansoureh Tavan[1*], Ali Azizi[1*], Hassan Sarikhani[1], Emran Dastres[2], Maria Manuela Rigano[3] and Mohammad Hossein Mirjalili[2]

Abstract

Background *Salvia multicaulis*Vahl is a medicinally valuable and ecologically sensitive species native to the Middle East. It is increasingly threatened by climate change and overharvesting. This study aimed to (1) predict the current (2025) and future (2050 and 2070) habitat suitability of *S. multicaulis* under two Shared Socioeconomic Pathways (SSP245 and SSP585) using MaxEnt model based on a set of climatic, topographic, and edaphic variables, (2) assess spatial variation in its phytochemical profiles, and (3) develop a quality zoning map integrating chemical and ecological data. A total of 35 occurrence records were compiled for ecological niche modeling, among which 17 representative populations were selected and analyzed for key bioactive compounds—ursolic acid, betulinic acid, oleanolic acid, total phenolics, flavonoids, and tannins—using HPLC and spectrophotometry.

Results Habitat modeling utilized 36 environmental predictors, with MaxEnt achieving a high mean AUC of 0.975. Principal component analysis, hierarchical clustering, and Pearson correlation analysis revealed distinct chemotypes and moderate correlations between compound concentrations and environmental factors, particularly soil organic carbon, nitrogen, temperature, and precipitation. Under future climate scenarios, suitable habitats are projected to shift northeast and southwest and fragment. Quantitatively, the total suitable habitat of *S. multicaulis* is projected to decline slightly (≈ − 2.5%) under SSP245–2050s, while modest expansions of ~ 1.8–4.3% are expected under higher-emission and long-term scenarios. Integration of habitat suitability and phytochemical richness revealed western and northwestern Iran as current hotspots for high-quality populations, while the north and northeastern regions may emerge as future refugia.

Conclusions These findings underscore the urgency of climate-informed conservation and cultivation planning for preserving both the ecological and pharmaceutical value of *S. multicaulis*, while supporting its sustainable harvesting from natural habitats.

Keywords Salvia multicaulis, MaxEnt model, Climate change, Habitat suitability, Quality evaluation

*Correspondence:
Mansoureh Tavan
mansuretavan@yahoo.com
Ali Azizi
azizi@basu.ac.ir

[1]Department of Horticultural Science, Faculty of Agriculture, Bu Ali Sina University, Hamedan 65174, Iran
[2]Department of Agriculture, Medicinal Plants and Drugs Research Institute, Shahid Beheshti University, Tehran 1983969411, Iran
[3]Department of Agricultural Sciences, University of Naples Federico II, Portici, Naples 80055, Italy

Introduction

The therapeutic efficacy of herbal medicines hinges on the complex interplay between the genetic potential of the source plant and the environmental conditions it experiences [1]. Medicinal plants, long valued in traditional remedies and increasingly important in modern pharmaceuticals, produce specialized metabolites responsible for their therapeutic effects [2]. While the synthesis of these metabolites is genetically programmed via enzyme-encoding genes and biosynthetic pathways, the environment exerts a significant influence on their final quantity and composition [3, 4]. In particular, environmental factors, including altitude, temperature, solar radiation, humidity and soil composition, contribute to substantial variations in active ingredient content across different geographical locations, ultimately determining the quality and effectiveness of the resulting herbal medicine [1, 5, 6].

Global climate change, combined with increasing human activity, significantly threatens the survival and distribution of valuable medicinal plants [4, 7, 8]. The altered climate patterns negatively affect their reproduction, growth, and spatial distribution, potentially leading to population decline and even extinction for some species [9]. To improve herbal medicine quality control, it is crucial to develop sophisticated analytical methods and establish robust models that link chemical composition to the ecological factors influencing plant growth. This understanding is vital for ensuring the consistent quality and safety of herbal medicine products [10].

Species distribution modeling (SDM) offers a powerful approach to understanding and predicting species' responses to climate change by forecasting potential distribution patterns based on existing data. While a variety of SDM algorithms are available, the maximum entropy model (MaxEnt) has emerged as a leading approach, largely due to its strong predictive capabilities [11–14]. MaxEnt is frequently utilized not only for forecasting species' spatial distributions, but also for assessing species-environment relationships through jackknife analysis [15–18]. Climate change projections are often represented by different scenarios called Shared Socioeconomic Pathways (SSPs), which describe possible future trajectories of greenhouse gas emissions, land use, and socio-economic developments. These scenarios include SSP126, representing a low emission pathway with strong mitigation; SSP245, a moderate emission scenario; SSP370, a high emission scenario with regional rivalry; and SSP585, representing a very high emission or worst-case trajectory. The development and narrative of these SSPs were established as a new framework for climate change research, integrating socioeconomic and climate projections to replace the previous Representative Concentration Pathways (RCPs) [19]. This integrated framework is crucial for the Coupled Model Intercomparison Project Phase 6 (CMIP6), which provides the foundational simulations for the IPCC's Sixth Assessment Report [20]. These pathways reflect varying degrees of global warming and associated environmental impacts. Incorporating multiple climate scenarios in species distribution modeling allows for a more comprehensive assessment of potential habitat changes under different futures, thereby improving the robustness of conservation and management strategies [21].

In parallel with SDM, machine learning approaches—including both correlative models such as MaxEnt and ensemble learners such as Random Forest—have become indispensable tools for capturing complex ecological and phytochemical patterns. MaxEnt, known for its robustness with presence-only data and effectiveness even with limited sample sizes, consistently achieves high accuracy in modeling habitat suitability for medicinal plants, often comparable to or exceeding ensemble methods [22]. Meanwhile, Random Forest offers distinct advantages in handling large, heterogeneous datasets and providing interpretable measures of variable importance, which are invaluable for identifying key environmental drivers of plant quality and distribution [23]. By integrating MaxEnt's niche modeling capabilities with Random Forest's predictive power and interpretability, researchers can generate highly accurate and nuanced quality zoning maps. This hybrid approach enhances the ability to forecast both the spatial distribution and phytochemical quality of medicinal species under diverse climate scenarios [24].

The influence of environmental conditions on the production of specialized metabolites in medicinal plants, which directly affect their ecological performance and distributional potential, underscores the importance of environmental variables in species distribution modeling (SDM). In this context, habitat suitability refers to the degree to which environmental conditions, such as climate, topography, and soil characteristics, support the survival, growth, and reproduction of a species within a given area. Understanding these relationships is essential for identifying suitable habitats under current conditions and forecasting potential range shifts under future climate scenarios. Despite increasing awareness of the effects of global climate change, the precise mechanisms through which it influences the phenological cycles, morphological traits, and therapeutic efficacy of medicinal plants remain incompletely elucidated. Developing robust models that integrate ecological and phytochemical data provides a foundation for identifying optimal cultivation regions and assessing the future distribution and quality of medicinal plants under changing climatic conditions [6].

Recent studies have successfully applied the MaxEnt model to predict the potential distribution of several medicinal and endemic species in Iran under various climate change scenarios. For example, Abolmaali et al. [25] modeled the habitat suitability of *Daphne mucronata* Royle, demonstrating the influence of topographic and climatic variables on its restricted distribution. Zare et al. [26] employed MaxEnt to identify suitable habitats and key environmental drivers for *Dorema ammoniacum* D. Don., emphasizing the strong association between precipitation gradients and species occurrence. Similarly, Noedoost et al. [27] investigated *Achillea eriophora* DC. and identified precipitation and temperature seasonality as key predictors, while Hosseini et al. [28] explored two *Thymus* species and emphasized the role of edaphic and bioclimatic factors. These findings collectively confirm the utility of MaxEnt for understanding the ecological requirements and conservation priorities of Iran's medicinal flora.

Salvia multicaulis Vahl, an endemic species of the Middle East with wild populations in various regions of Iran [29], is recognized as a source of precious specialized metabolites [30–32]. These metabolites, including diterpenoids, norditerpenoids, triterpenoids, salvimultine, phenolic compounds, and essential oil, are responsible for the plant's notable pharmacological activities. Research has demonstrated that *S. multicaulis* exhibits antimicrobial, antioxidant, anti-inflammatory, antiangiogenic, wound healing, and cytotoxic properties [30, 31, 33, 34]. This plant naturally occurs at mid- to high-elevations on grassy mountain slopes, hillsides, and riverbanks, occupying approximately the mountainous regions spanning central, western, and northwestern Iran, under diverse climatic and edaphic conditions [35, 36]. Increasing demand for medicinal raw materials, combined with climate change and land-use pressures, is likely threatening wild populations and reducing habitat integrity [37].

Research on *S. multicaulis* has primarily focused on its pharmacological properties and phytochemical composition [31, 32, 34], whereas limited attention to its habitat suitability and the impact of environmental factors on quality variation [38]. The effects of climate change on the distribution of *S. multicaulis* and the relationships between its chemical profiles and environmental variables are also poorly understood. This study introduces an integrated analytical framework that combines species distribution modeling with phytochemical profiling to jointly assess habitat suitability and medicinal quality of *S. multicaulis* under present and projected climatic conditions. By linking ecological and chemical dimensions, this research moves beyond conventional single-aspect studies and provides new insights into how environmental drivers shape both the spatial distribution and bioactive potential of the species. The proposed approach offers a practical basis for identifying climate-resilient and high-quality habitats, supporting more informed conservation and sustainable management strategies for medicinal plants facing ongoing environmental change.

This study aims to address these gaps by (1) estimating the current habitat suitability of *S. multicaulis* under present climatic conditions and predicting its potential distribution under future climate scenarios using MaxEnt modeling and GIS, (2) analyzing triterpenic acids (TAs), including ursolic acid (UA), betulinic acid (BA), and oleanolic acid (OA), and phenolics such as total phenol (TPC), total flavonoid (TFC), and total tannin (TTC) contents of samples using HPLC and spectrophotometry, and (3) exploring the correlations between chemical composition, ecological factors, and product quality using chemometric analysis and multivariable statistics. Finally, a comprehensive quality zoning map of *S. multicaulis* will be developed using R software (version 4.4.3), based on the established relationships, with a particular focus on how do environmental variables influence the phytochemical composition of *S. multicaulis* across its range?

Materials and methods

Study area

The study area is located in the western and northwestern regions of Iran, encompassing parts of Alborz, West Azerbaijan, Kordestan, Zanjan, Ghazvin, Hamadan, Lorestan, Kermanshah, and Markazi provinces (Fig. 1). Geographically, it spans latitudes approximately between 33°52′ to 38°30′ N and longitudes 45°00′ to 51°20′ E (approximately 130000 km^2).

This region falls within the Zagros Mountain Range, one of Iran's primary geomorphological units, and is characterized by rugged topography, with elevations ranging from 1,200 m to over 2,500 m above sea level. Vegetation is characterized by a mosaic of open woodlands, shrublands, and steppe communities with 35–60% plant cover, depending on slope and grazing intensity. The dominant life forms are phanerophytes, chamaephytes, and hemicryptophytes, reflecting adaptation to semi-arid montane conditions [39]. The dominant arboreal species include *Quercus castaneaefolia* C. A. Mey, *Pistacia atlantica* Desf., *Juniperus excelsa* M.Bieb., and *Amygdalus scoparia* Soach, accompanied by shrubs such as *Astragalus* spp., *Acantholimon* spp., *Berberis vulgaris* L., and *Centaurea* spp. Herbaceous vegetation mainly comprises perennial grasses (*Stipa*, *Bromus*, *Festuca*) and medicinal forbs like *Thymus* spp. and *Ferula* spp., reflecting the typical semi-arid montane steppe flora of western Iran [28]. The topographic complexity results in diverse microclimatic conditions, contributing to the formation of varied ecological niches suitable for the growth of *S.*

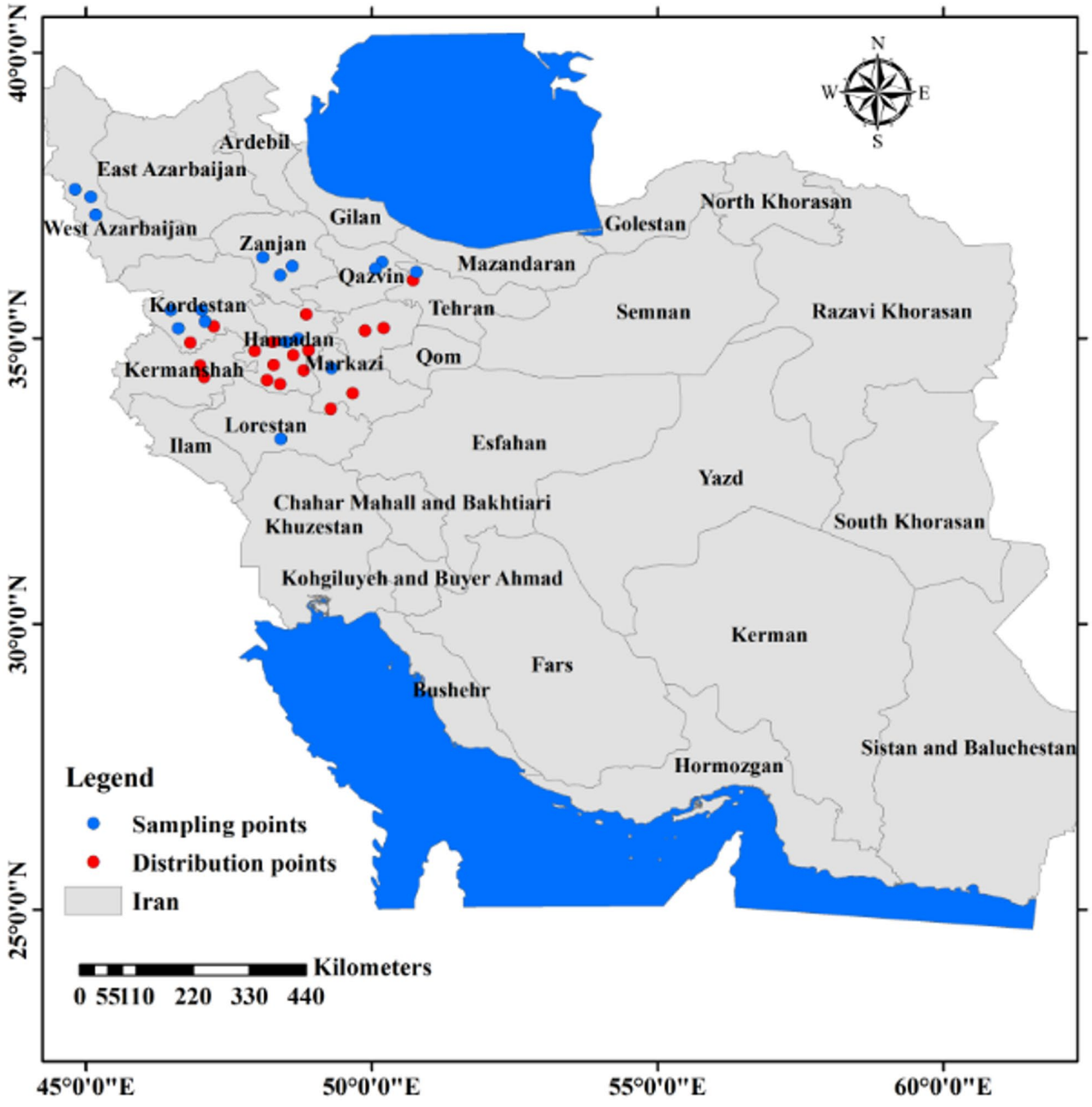

Fig. 1 Geographical distribution points and sampling points of *Salvia multicaulis* in Iran using Arc-map 10.8.1 software (URL: https://www.arcgis.com/index.html)

multicaulis [28]. The prevailing climate is temperate to cold semi-arid, with cold winters and relatively dry summers. Annual precipitation varies between 300 mm and 1,200 mm, while mean annual temperatures range from – 4 °C to 8.5 °C, depending on altitude and aspect [40].

Soils in this region are generally calcareous, with moderate to high levels of organic carbon and nitrogen, which are key edaphic factors influencing the biosynthesis of secondary metabolites in medicinal plants. The selected area encompasses a mixture of montane slopes, valleys, and foothills, reflecting a high degree of environmental heterogeneity. Such variability makes this zone particularly suitable for investigating the interactions between climatic and edaphic variables and their influence on both habitat suitability and phytochemical quality.

Overall, the selected region provides a representative natural laboratory for modeling the current and future distribution of *S. multicaulis*, as well as for evaluating spatial patterns in the accumulation of its bioactive compounds under shifting environmental conditions.

Geographic distribution areas of samples

Data on the distribution of *S. multicaulis* populations were gathered through field studies in its primary habitats, supplemented by information from published literature (Fig. 1). A total of 35 occurrence points for *S. multicaulis* were compiled for this study. Of these, 18 points were obtained from published literature [38, 41], while the remaining 17 were collected through systematic field surveys. To minimize spatial autocorrelation, a minimum distance filter of 1 km was applied between all points. This final set was selected to capture the full ecological and geographical range of the species within the study area. The species' endangered status, combined with threats from drought and over-harvesting, necessitated targeting locations representing critical environmental gradients [37]. This design ensures both scientific robustness and conservation relevance for habitat suitability and phytochemical quality modeling.

From these 35 sites, 17 representative populations were selected for phytochemical analysis based on accessibility, population size, and habitat integrity. Plant materials from these 17 sites (Fig. 1) were identified by Dr. Ranjbar from the Department of Biology, Bu-Ali Sina University, Hamedan, Iran. All field investigations and plant material collections were conducted between 2021 and 2025, in full compliance with local and national regulations. Specifically, the collections followed the guidelines and protocols established by the Iranian Department of Environment (DOE) and relevant provincial agricultural authorities to ensure ethical and legal compliance. No additional permits or licenses were required. The dried plants and voucher specimens (Number: A-Hort-97-SMP) were deposited at the Bu-Ali-Sina University Herbarium. The dried aerial parts of the samples were powdered, and 0.5 g of each was prepared for extraction. The resulting extracts were collected, stored in sealed glass vials at 4 °C, and subsequently analyzed via high-performance liquid chromatography (HPLC). To reduce spatial autocorrelation, occurrence points were spatially thinned using the thinData() function with a 1 km distance threshold, consistent with the resolution of environmental predictors. After thinning, 35 unique presence records were retained for modeling. Furthermore, habitat suitability analysis was conducted using 35 records compiled from field investigations and a literature review.

Methodology

An integrated methodological framework, combining ecological data collection with machine learning approaches, was employed to model the current and future habitat suitability and phytochemical quality of *S. multicaulis*. The framework encompasses several sequential steps, from data mining and preprocessing to habitat and quality modeling, binary mapping, and final integration of outputs, as illustrated in Fig. 2.

Chemical composition analysis

The total phenol (TPC), total flavonoid (TFC), and total tannin (TTC) contents were quantified spectrophotometrically using the methods of Ainsworth and Gillespie [42], Kamtekar et al. [43], and Galvão et al. [44], respectively.

The quantification of triterpenic acids (TAs), including ursolic acid (UA), betulinic acid (BA), and oleanolic acid (OA), was performed using HPLC, following the protocol described by Tavan et al. [32]. Identification of the compounds was achieved by comparing their retention times with those of authentic standards. The concentrations of the individual compounds were determined based on their respective standard calibration curves. A detailed description of all analytical methods is provided in the Supplementary Material.

Statistical analyses of the phytochemical data were conducted to complement the laboratory measurements. All experiments were conducted in triplicate, and the results are presented as mean ± standard deviation (SD). Statistical analyses were performed using R software (version 4.4.3). Differences among means were assessed using Duncan's multiple range test at a significance level of $p < 0.05$. Pearson correlation analysis, principal component analysis (PCA), heat map analysis, were generated via R software (version 4.4.3). PCA was used to summarize the variance among phytochemical compounds and visualize the overall structure of the data. Cluster and heat map analyses were conducted to explore similarity patterns among populations based on compound concentrations.

Correlation analysis between the chemical components and ecological factors

To investigate the influence of ecological variables on the accumulation of bioactive compounds, ecological data corresponding to the sampling locations were extracted using R software (version 4.4.3), based on the geographic coordinates (longitude and latitude) of each site. Subsequently, Pearson correlation analysis was performed to examine pairwise linear relationships between six key bioactive compounds (TPC, TFC, TTC, UA, BA, and OA) and 16 environmental factors (as listed in Table 1). The strength of Pearson correlation coefficients (r) was categorized as follows: $|r| > 0.50$ was considered a strong correlation, $|r| = 0.30–0.50$ a moderate correlation, and $|r| = 0.10–0.30$ a weak correlation [45]. The resulting correlations were further integrated with the predicted habitat suitability map of *S. multicaulis* to develop a spatial zoning map illustrating the medicinal quality distribution of the samples across the studied regions.

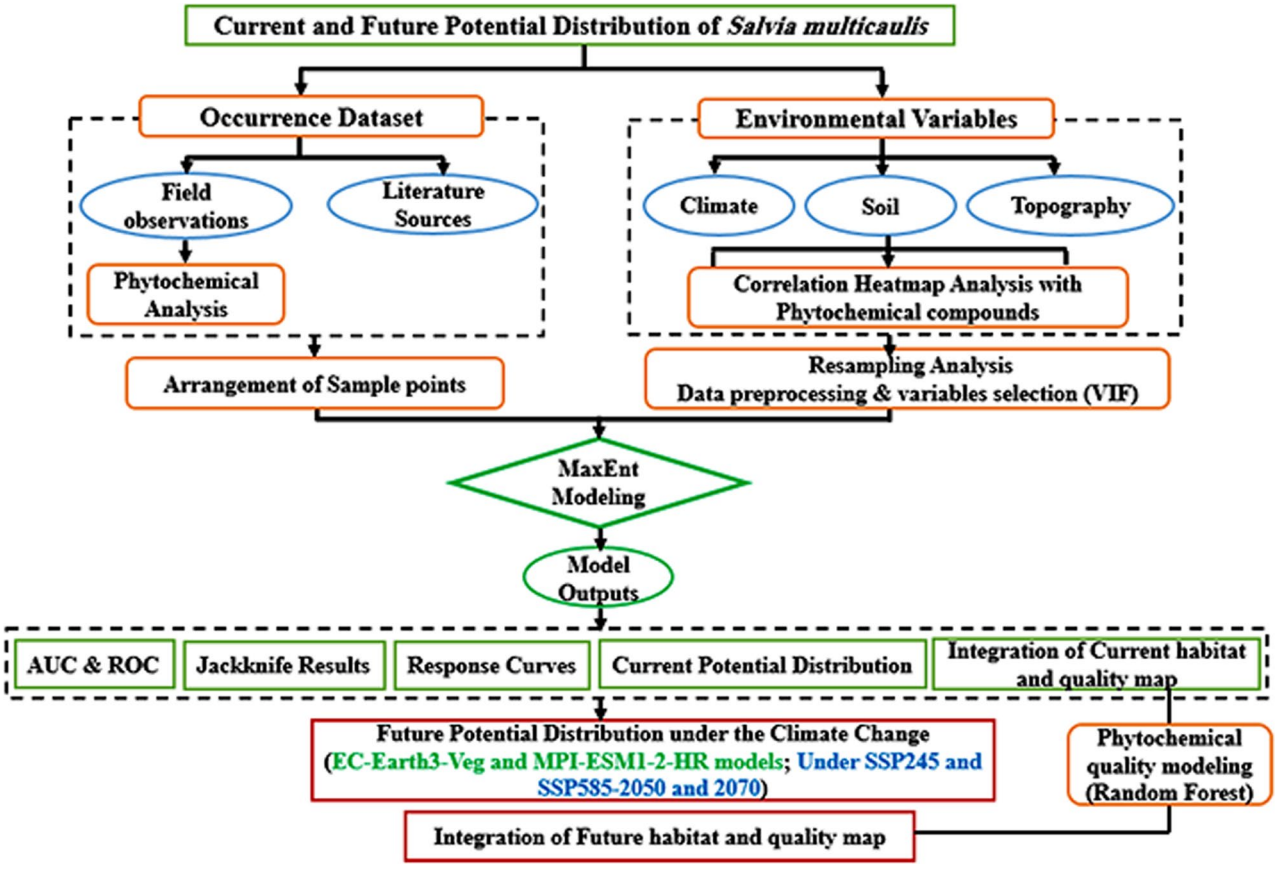

Fig. 2 Flowchart of methodology

Environmental variables

To model habitat suitability for *S. multicaulis*, 36 environmental predictors related to plant growth were used (Table 1). These included 19 bioclimatic variables, 12 solar radiation measures, two soil variables (soil organic carbon and Nitrogen), and three topographic parameters (elevation, slope, and aspect). Bioclimatic and solar radiation data, with a 30-second spatial resolution, were obtained from the WorldClim v2.1 database (https://www.worldclim.org). Soil variables were derived from the ISRIC SoilGrids v2.0 database (www.soilgrid.org; www.isric.org). Topographic information, including elevation, slope, and aspect, was derived from a 30-meter resolution digital elevation model (DEM) using the surface analysis tools in ArcGIS.

Among the available CMIP6 models, EC-Earth3-Veg and MPI-ESM1-2-HR were selected because they have demonstrated superior performance and reliability in simulating key climatic variables across Iran in recent model-evaluation studies [46–49]. Their inclusion thus provides a regionally optimized basis for assessing the future habitat suitability of *S. multicaulis* under different climate scenarios. For future projections, bioclimatic variables were derived from the EC-Earth3-Veg and MPI-ESM1-2-HR models under two Shared Socioeconomic Pathways (SSPs), SSP245 and SSP585, representing intermediate and high-emission trajectories, respectively. These datasets correspond to two future time horizons: 2041–2060 (mid-century; hereafter 2050) and 2061–2080 (late-century; hereafter 2070). The SSPs framework provide improved representation of greenhouse gas concentration trajectories and socio-economic drivers compared to previous RCP-based scenarios, enhancing the realism of future climate simulation [19–21]. Environmental parameters were resampled to a spatial resolution of 2.5 arc-minutes (approximately 4.5 × 4.5 km^2).

Species distribution modelling process

The species distribution modelling workflow commenced with an assessment of multicollinearity among the environmental predictors. Variance Inflation Factor (VIF) analysis was performed to identify and exclude redundant variables. A conservative threshold of VIF >10 was applied, in accordance with established statistical guidelines, to eliminate predictors with high multicollinearity that could distort model interpretation and stability [50, 51].

Out of the initial 36 environmental variables, 16 predictors with VIF values below the threshold were retained for subsequent modelling (Table 1). These retained variables were included in the final models (marked as "Yes"

Table 1 Environmental variables used in maxent model

Variable code	Variable name	Unit	Mean ± SD	Data source	Model
bio 1	Annual Mean Temperature	℃	11.34 ± 2.31	WorldClim 2.1 database (https://www.worldclim.org)	Yes
bio2	Mean Diurnal Range (Mean of monthly (max temp - min temp))	℃	14.15 ± 1.47		Yes
bio3	Isothermality (bio 2/bio 7) (*100)	%	35.22 ± 2.81		No
bio4	Temperature Seasonality (SD *100)	℃	945.85 ± 31.29		Yes
bio5	Max Temperature of Warmest Month	℃	33.16 ± 2.92		No
bio6	Min Temperature of Coldest Month	℃	−6.95 ± 2.33		No
bio7	Temperature Annual Range (bio5-bio6)	℃	40.12 ± 1.52		No
bio8	Mean Temperature of Wettest Quarter	℃	4.60 ± 3.02		Yes
bio9	Mean Temperature of Driest Quarter	℃	22.51 ± 2.23		Yes
bio10	Mean Temperature of Warmest Quarter	℃	22.90 ± 2.29		No
bio11	Mean Temperature of Coldest Quarter	℃	−0.42 ± 2.52		No
bio12	Annual Precipitation	mm	390.94 ± 93.17		Yes
bio13	Precipitation of Wettest Month	mm	70.94 ± 18.56		No
bio14	Precipitation of Driest Month	mm	2.18 ± 1.81		Yes
bio15	Precipitation Seasonality (Coefficient of Variation)	mm	73.20 ± 7.14		Yes
bio16	Precipitation of Wettest Quarter	mm	180.59 ± 47.40		No
bio17	Precipitation of Driest Quarter	mm	8.00 ± 6.36		No
bio18	Precipitation of Warmest Quarter	mm	12.82 ± 9.34		Yes
bio19	Precipitation of Coldest Quarter	mm	148.24 ± 45.71		No
DEM	Elevation	m	1776.94 ± 343.85	Spatial analysis module in ArcMap 10.3	Yes
Slope	Slope	°	28.22 ± 3.22		Yes
TRASP	Aspect	°	0.50 ± 0.36		Yes
Srad1	Monthly mean solar radiation for January	$kJ{\cdot}m^{-2}{\cdot}day^{-1}$		WorldClim 2.1 database (https://www.worldclim.org)	No
Srad2	Monthly mean solar radiation for February	$kJ{\cdot}m^{-2}{\cdot}day^{-1}$	11240.24 ± 577.44		No
Srad3	Monthly mean solar radiation for March	$kJ{\cdot}m^{-2}{\cdot}day^{-1}$	13920.65 ± 620.83		No
Srad4	Monthly mean solar radiation for April	$kJ{\cdot}m^{-2}{\cdot}day^{-1}$	17549.24 ± 391.86		No
Srad5	Monthly mean solar radiation for May	$kJ{\cdot}m^{-2}{\cdot}day^{-1}$	21870.41 ± 510.75		No
Srad6	Monthly mean solar radiation for June	$kJ{\cdot}m^{-2}{\cdot}day^{-1}$	26488.41 ± 860.58		Yes
Srad7	Monthly mean solar radiation for July	$kJ{\cdot}m^{-2}{\cdot}day^{-1}$	26195.41 ± 764.89		No
Srad8	Monthly mean solar radiation for August	$kJ{\cdot}m^{-2}{\cdot}day^{-1}$	23575.18 ± 755.66		Yes
Srad9	Monthly mean solar radiation for September	$kJ{\cdot}m^{-2}{\cdot}day^{-1}$	20322.24 ± 909.89		No
Srad10	Monthly mean solar radiation for October	$kJ{\cdot}m^{-2}{\cdot}day^{-1}$	14528.18 ± 882.12		No
Srad11	Monthly mean solar radiation for November	$kJ{\cdot}m^{-2}{\cdot}day^{-1}$	10217.47 ± 532.13		No
Srad12	Monthly mean solar radiation for December	$kJ{\cdot}m^{-2}{\cdot}day^{-1}$	8106.82 ± 536.67		No
Nitrogen	Nitrogen	%N	1.51 ± 0.32	World Soil Information Database (www.soilgrid.org; www.isric.org)	Yes
SOC	Soil organic carbon	% weight	6.89 ± 4.01		Yes

in Table 1), while the remaining predictors ("No") were excluded due to high collinearity. The VIF values for retained environmental predictors have been provided in Table S2.

Species occurrence probabilities were estimated using the MaxEnt algorithm, a machine learning method that integrates statistical modelling principles. MaxEnt (versions 1.0–3) was implemented within the R statistical environment (version 4.4.3) via the "dismo" package (version 1.3–9). Model calibration and validation were conducted using tenfold cross-validation, in which the occurrence dataset was randomly partitioned into ten subsets; nine were used for training and the remaining one for testing in each run. To further enhance model robustness and ensure adequate sampling of environmental variability, the modelling procedure was repeated in ten independent replicates, each using 10,000 background points. This number is sufficiently large to robustly characterize the available environmental space and reduce sampling bias, a common practice in MaxEnt

modeling [28, 52]. An optimal prediction threshold was determined from the balance between sensitivity and specificity metrics [52].

Model performance was evaluated using the Receiver Operating Characteristic (ROC) curve, with the Area Under the Curve (AUC) statistic serving as a threshold-independent measure of discriminatory capacity. AUC values were interpreted as follows: 0.9–1.0, excellent; 0.8–0.9, good; 0.7–0.8, fair; 0.6–0.7, poor; and < 0.6, model failure. This classification is widely adopted in ecological niche modeling and aligns with established ecological literature [53]. To determine the relative influence of each environmental variable on species distribution under current climatic conditions, the Jackknife test was applied alongside percent contribution (PC) and permutation importance (PI) metrics. Response curves were then generated for the most influential predictors, identified based on their percent contribution and Jackknife test performance. These criteria enabled identification of the environmental variables exerting the strongest influence on the potential distribution and phytochemical quality of *S. multicaulis*.

Finally, a single MaxEnt model was retrained using the complete occurrence dataset and the selected environmental predictors to generate spatial predictions of habitat suitability under both present and projected future climate scenarios. All modelling and map generation were performed in R (version 4.4.3).

Furthermore, to model the spatial distribution of phytochemical quality, the Random Forest (RF) algorithm was applied separately to each of the six measured compounds: UA, BA, OA, TPC, TFC, and TTC. Predictor variables included the same environmental dataset used in the MaxEnt modeling, reduced by multicollinearity analysis. RF models were implemented in R using the randomForest package (Liaw & Wiener, 2002). Given the limited sample size ($n = 17$), which increases the risk of overfitting with complex tuning procedures, we employed the following established and computationally efficient settings: The number of trees (ntree) was set to 500 to ensure the stabilization of the Out-of-Bag (OOB) error. The number of variables available for splitting at each tree node (mtry) was set to the package default for regression (p/3, resulting in 5 with our 16 predictors), and the minimum node size (nodesize) was also left at its default value of 5. These default settings are widely accepted and provide a good balance between predictive performance and model robustness. The trained RF models were then applied using the predict function to each raster pixel across the study area (at the same resolution and CRS as the MaxEnt habitat suitability maps) to generate continuous spatial prediction maps for each compound. If necessary, rasters were resampled to match the MaxEnt outputs.

To evaluate the predictive performance and reduce potential overfitting given the limited sample size ($n = 17$), RF models were trained for each phytochemical compound (UA, BA, OA, TPC, TFC, and TTC) using 10-fold cross-validation. The environmental predictors included 16 reduced variables selected after VIF screening (MyExpl_Reduced). Model accuracy was quantified by the coefficient of determination (R^2), root mean square error (RMSE), and mean absolute error (MAE). Variable importance was assessed using the permutation-based %IncMSE metric, which quantifies the relative contribution of each predictor to model performance. All computations were conducted in R using the randomForest and caret packages, and outputs were saved as summarized tables and raster prediction maps for each compound.

To identify areas combining high habitat suitability and high phytochemical quality, the continuous RF-derived quality maps were integrated with the continuous habitat suitability map generated by MaxEnt. To produce the combined quality maps, each compound-specific raster was multiplied by the MaxEnt suitability raster to retain values only in suitable habitat areas. The six compound-specific combined rasters were then averaged on a per-pixel basis using the arithmetic mean to create a continuous mean map.

The continuous mean combined map was subsequently classified into four distinct categories using the Jenks Natural Breaks optimization algorithm (Jenks, 1967) [54], which objectively determines class boundaries by minimizing within-class variance and maximizing between-class variance. This data-driven classification yielded the following categories: No suitability (0–0.2), Low suitability (0.2–0.4), Medium suitability (0.4–0.6), and High suitability (0.6–1). This classification scheme follows established practices in species distribution and habitat suitability modeling [1, 55]. The chosen breaks provide a clear and ecologically meaningful interpretation of the model's output, effectively distinguishing between non-habitat, marginal habitat, and core habitat areas. This final classified mean map was used to delineate priority areas for *S. multicaulis* conservation and cultivation under both current and projected future climate conditions.

Results

Phytochemical profiling and multivariate analysis of *S. multicaulis* samples

The concentrations of three triterpenoids—UA, BA, and OA—alongside TPC, TFC, and TTC were quantified in 17 *S. multicaulis* samples (Table S1). Principal Component Analysis (PCA) was performed to reduce the dimensionality of the data and to identify the main components explaining the variance among populations (Fig. 3A). The first two principal components, PC1 and

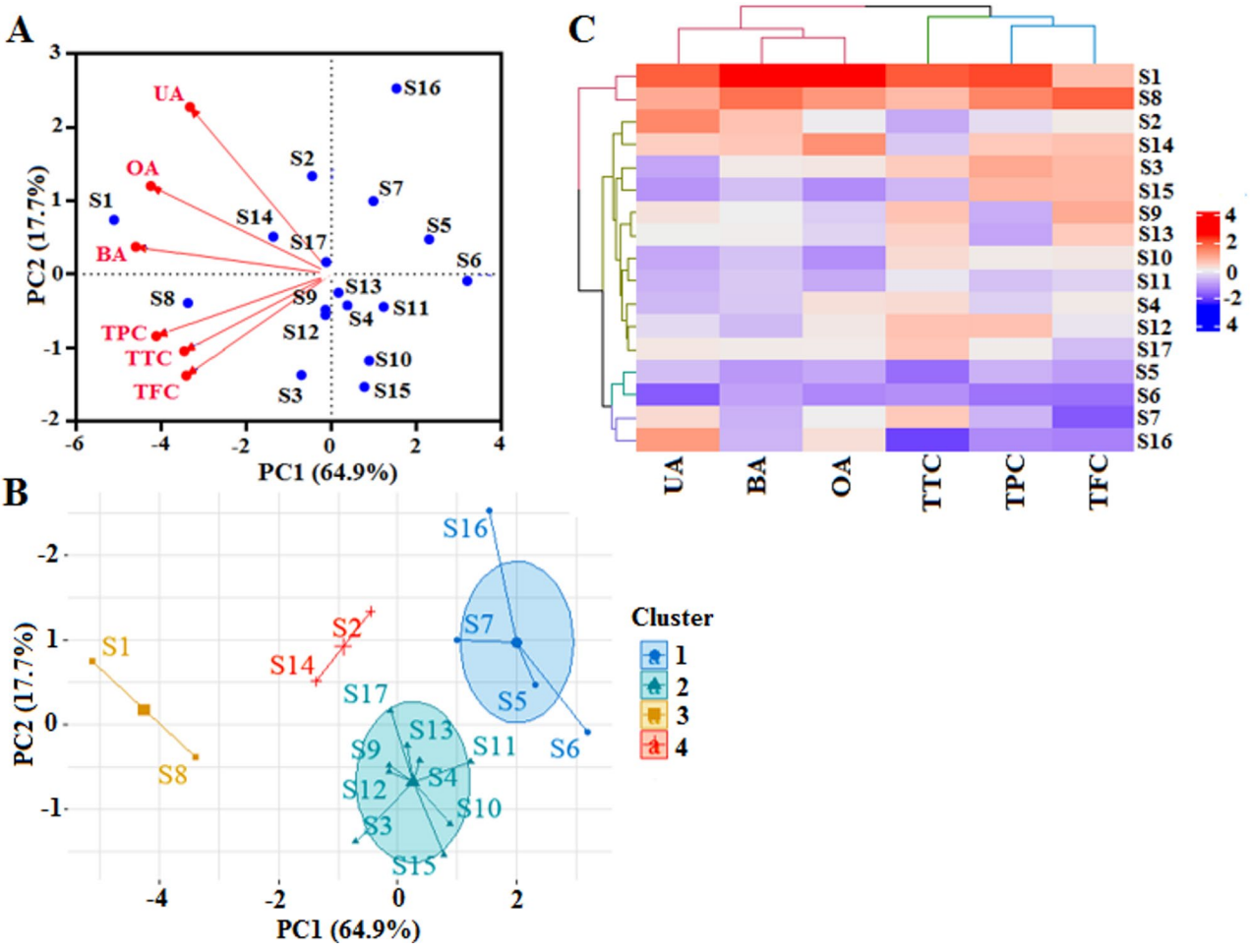

Fig. 3 Principal component analysis (**A**), cluster plot (**B**), and hierarchical heatmap (**C**) for *Salvia multicaulis* samples

PC2, accounted for 64.9% and 17.7% of the total variance, respectively, summing to 82.6%. This high cumulative variance indicates robust dimensionality reduction and effective visualization of phytochemical variation. The PCA biplot revealed distinct spatial separation among samples, suggesting a strong influence of geographic origin on phytochemical composition. PC1 mainly represented the phenolic–triterpenoid contrast, while PC2 was dominated by variation in UA and OA, indicating two major biochemical axes explaining phytochemical differentiation among the populations. Samples from S3 (Najdaresi-West Azerbaijan), S8 (Gazan-Kordestan), S9 (Asadabad-Hamedan), and S12 (Jaidasht-Ghazvin) were aligned negatively along PC1, showing strong negative associations with phenolic-related traits (TPC, TFC, TTC). In contrast, samples from S1 (Taleghan-Alborz), S2 (Khangah sorkh-West Azerbaijan), S14 (Zaghe-Lorestan), and S17 (Ghidar-Zanjan) were located positively along PC2, exhibiting strong correlations with UA, OA, and BA—highlighting triterpenoid dominance in these regions. Other samples demonstrated weaker or non-specific associations, indicating the presence of diverse putative chemotypic responses to environmental conditions.

To evaluate the similarity structure among populations based on their phytochemical profiles and further validate these findings, a K-means cluster plot based on the same two principal components (PC1 and PC2) was generated (Fig. 3B), revealing clear putative chemotypic groupings among the samples. Four distinct clusters were identified: Cluster I included S1 and S8, which were associated with uniformly high concentrations of all six compounds; Cluster II comprised S2 and S14, characterized by elevated triterpenoid levels with lower phenolic content; Cluster III included S5 (Sural-Kordestan), S6 (Tazeabad-Kordestan), S7 (Darenashur-Kordestan), and S16 (Abdal-Zanjan), which demonstrated intermediate levels of all compounds; while the remaining populations formed Cluster IV, displaying variable but generally lower compound concentrations. These groupings support the existence of chemical ecotypes with shared biosynthetic tendencies.

Complementing these analyses, a hierarchical heatmap (Fig. 3C) was generated to visualize the distribution

patterns and relative concentrations of the phytochemical compounds across different geographical regions. This analysis further grouped the 17 populations into four major putative chemotypic clusters based on similarities in compound abundance. Cluster I (S1 and S8) displayed consistently high levels of all measured phytochemicals and represents the most chemically enriched group. Cluster II (S5 and S6) exhibited uniformly low compound levels, indicating a weak phytochemical profile. Cluster III (S7 and S16) showed moderate concentrations across traits, suggesting a chemically intermediate status. Cluster IV encompassed the remaining samples, characterized by heterogeneous phytochemical patterns with generally moderate to low compound levels. This clustering reinforces the high degree of chemical heterogeneity among populations and underscores the presence of site-specific chemotypes. Particularly, the identification of highly enriched groups such as Cluster I offers valuable guidance for future conservation, cultivation, and targeted phytochemical exploitation.

Relationship between phytochemical composition and environmental factors

As shown in Fig. 4, a correlation exists between phytochemical contents and the surrounding environmental variables. Pearson correlation analysis indicated moderate positive associations between the contents of BA, OA, TPC, and TFC and soil organic carbon (SOC), suggesting a potential role of organic matter in enhancing phytochemicals accumulation. Correlations suggest

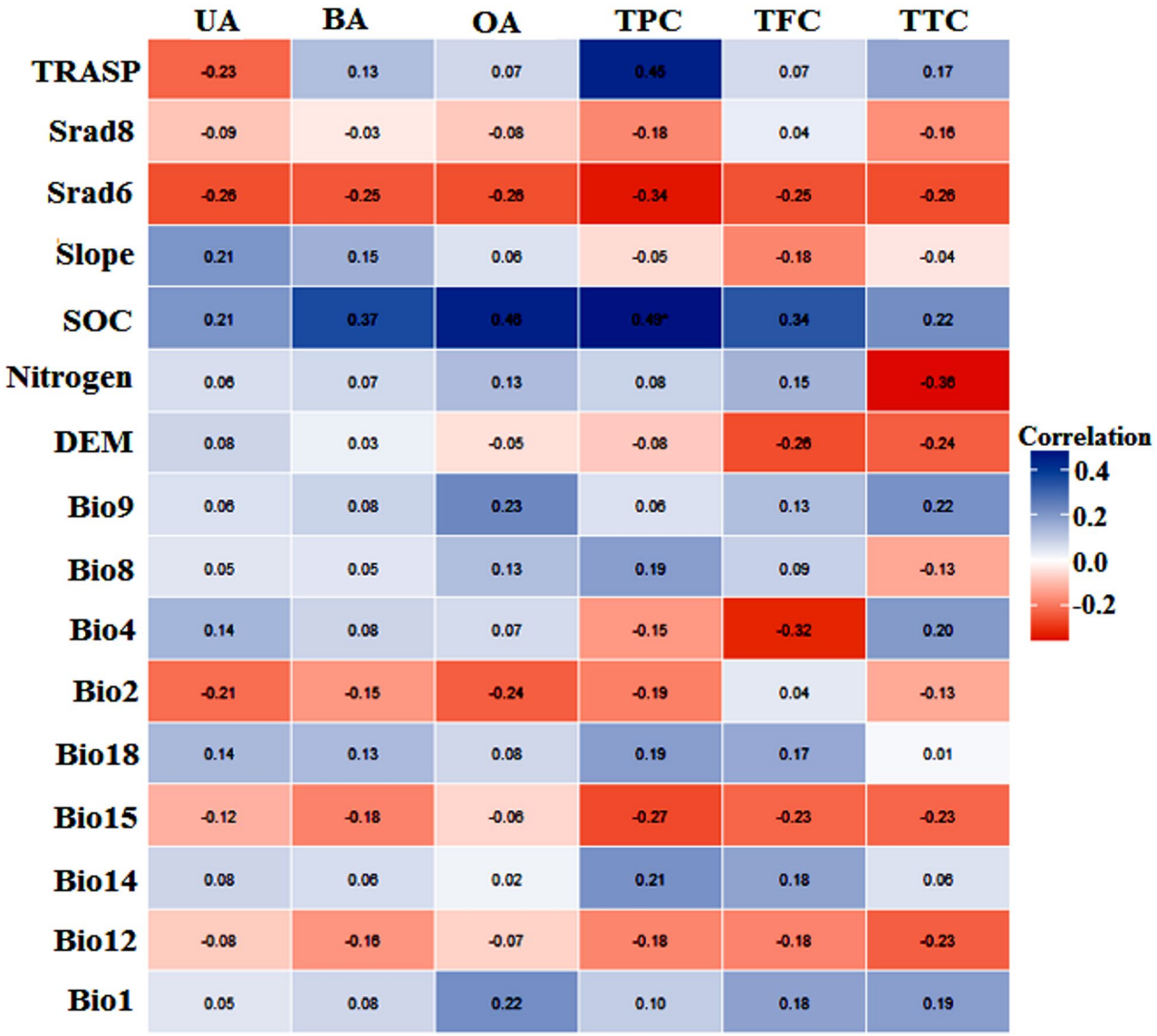

Fig. 4 Correlation heatmap between chemical composition and environmental variables. Ursolic acid (UA), betulinic acid (BA), oleanolic acid (OA), total phenol (TPC), total flavonoid (TFC), and total tannin (TTC) contents

environmental influences but do not imply causation. Additionally, among the tested associations, only the correlation between SOC and TPC was statistically significant ($r = 0.49$, $p < 0.05$), while all other correlations did not reach significance. TPC also exhibited a moderate positive correlation with TRASP ($r = 0.45$), as well as weak positive correlations with mean temperature of wettest quarter (Bio8, $r = 0.19$), precipitation of warmest quarter (Bio18, $r = 0.19$), and precipitation of driest month (Bio14, $r = 0.21$). Furthermore, OA content exhibited weak correlations with annual mean temperature (Bio1, $r = 0.22$), mean temperature of driest quarter (Bio9, $r = 0.23$), Nitrogen content ($r = 0.13$), and mean temperature of wettest quarter (Bio8, $r = 0.13$). The UA content was weakly associated with slope ($r = 0.21$), SOC ($r = 0.21$), and temperature seasonality (Bio4, $r = 0.14$) and precipitation of warmest quarter (Bio18, $r = 0.14$), suggesting that both topographic factors and seasonal climatic conditions may influence its biosynthesis. Similarly, TTC content was positively correlated with TRASP ($r = 0.17$), SOC ($r = 0.22$), and a suite of temperature-related variables including Bio9 ($r = 0.22$), Bio4 ($r = 0.20$), and Bio1 ($r = 0.19$). These findings highlight the complex interplay between climatic, edaphic, and topographic factors in modulating the phytochemical profile of *S. multicaulis*.

MaxEnt model evaluation

The ROC curve is a widely utilized metric for assessing the performance of binary classification models [1]. In the present study, the ROC analysis of the MaxEnt model demonstrated robust predictive performance across both the training and test datasets (Fig. S1). The model achieved a mean AUC value of 0.975 over ten replicate runs, indicating an excellent level of accuracy and reliability.

Environmental variable contributions and response patterns

During the current period, fourteen environmental variables were identified as the most influential predictors of *S. multicaulis* distribution: Bio1, Nitrogen, Bio12, Srad6, Srad8, Slope, Bio14, Bio15, TRASP, DEM, Bio2, SOC, Bio18, and Bio8. These variables contributed 30.2%, 13.8%, 12.7%, 10.2%, 9.4%, 5.2%, 4.9%, 3.9%, 3.4%, 3.2%, 1.6%, 0.7%, 0.6%, and 0.1% to the model, respectively. Their corresponding permutation importance values were 23.5%, 0.1%, 0.4%, 0.0%, 1.0%, 1.1%, 23.3%, 35.6%, 3.2%, 4.5%, 4.1%, 2.4%, 0.1%, and 0.5%, respectively (Fig. 5A). In MaxEnt, percent contribution is path-dependent and reflects the incremental gain attributed to each predictor during model training, whereas permutation importance quantifies the model's reliance on each predictor in the final prediction by measuring performance loss after permuting its values. Consequently, the two metrics may diverge, especially when predictors share information. The jackknife test further confirmed the dominant role of annual mean temperature (Bio1), which produced the highest regularized training gain when used in isolation, indicating its unique and substantial contribution to model performance (Fig. 5B).

Response curves for the most influential variables, identified based on percent contribution and Jackknife test results, highlight the distinct ecological preferences of *S. multicaulis* (Fig. 6). It is generally accepted that environmental variable ranges corresponding to a predicted presence probability above 0.5 indicate ecologically suitable conditions that support the growth, survival, and distribution of the species [4, 56]. For Bio1 (annual mean temperature), the suitable range for *S. multicaulis* occurrence spans approximately – 4 °C to 8.5 °C, with maximum suitability areas centered around 7.5 °C. Suitability declines sharply outside this interval, indicating a preference for cool-temperate climates typically associated with higher altitudes or mountainous regions.

The response curve for soil nitrogen reveals a positive correlation between nitrogen availability and the predicted presence of the species. Habitat suitability increases steadily with nitrogen levels, reaching a plateau around 1.2, which corresponds to the maximum predicted presence probability ($p \approx 1.0$). Beyond this threshold, suitability remains consistently high, suggesting a tolerance for moderate to high nitrogen conditions without evidence of decline at elevated concentrations. Regarding annual precipitation (Bio12), the response curve indicates that the predicted presence probability exceeds 0.55 across a broad precipitation range, starting at approximately 300 mm/year and remaining high up to 1,200 mm/year. This pattern implies that *S. multicaulis* is adapted to moderate to high precipitation regimes, exhibiting ecological plasticity under varying rainfall conditions. The absence of a marked decline at higher precipitation levels suggests tolerance to wetter environments, while values below 300 mm appear suboptimal.

According to the response curve for solar radiation in June (Srad6), the predicted probability of *S. multicaulis* presence exceeds 0.55 across a relatively broad range, approximately from 20,000 to 29,000 $kJ \cdot m^{-2} \cdot day^{-1}$. The highest habitat suitability ($p \approx 1$) is observed around 28,000 $kJ \cdot m^{-2} \cdot day^{-1}$. This pattern suggests that *S. multicaulis* prefers moderate to moderately high solar radiation levels in June, which may be critical for optimal photosynthetic activity and secondary metabolite production during its active growth period. For precipitation seasonality (Bio15), the species shows its highest predicted presence probability ($p > 0.55$) within a coefficient of variation range of approximately 22 to 75 mm. This indicates a preference for habitats with moderate rainfall

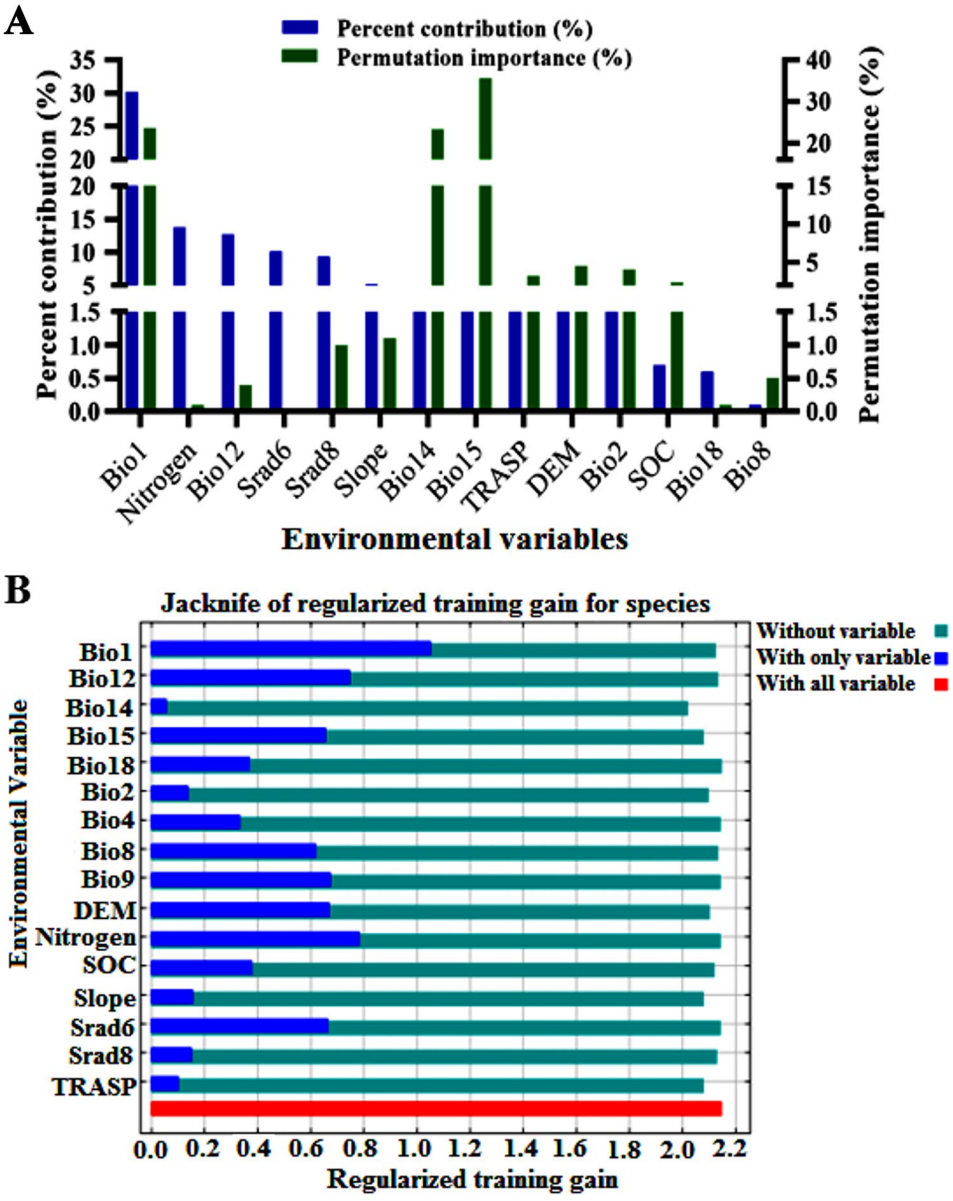

Fig. 5 Contribution and permutation importance of key environmental variables in the final model (**A**), Jackknife testing of environmental variables (regularized training gain) (**B**)

variability, while a steep decline in suitability beyond 90 mm suggests sensitivity to extreme precipitation fluctuations, potentially limiting the species' distribution in highly erratic climates.

Current potential distribution and quality zonation estimates

The results of the MaxEnt simulation revealed the potential geographical distribution of *S. multicaulis* under current climatic conditions (Fig. 7A). According to the criteria of habitat suitability zoning, the high- and medium-suitability zones cover areas of 73517.47 km^2 and 47648.20 km^2, respectively, whereas the low-suitable and unsuitable zones cover 1494090.47 km^2. The model identified high-altitude regions, including Hamadan, Kordestan, West Azerbaijan, Markazi, Qazvin, and Kermanshah, as the primary areas of highly suitable habitat for the species. The significant extrapolation of the predicted potential distribution beyond the known occurrence range (Fig. 7A) is a common outcome in species distribution modeling. This pattern can theoretically be attributed to two main factors: (1) the model identifies all areas that are climatically and topographically suitable at the specific resolution of the environmental data used, which may not capture fine-scale barriers; and (2) the actual realization of this potential is constrained by

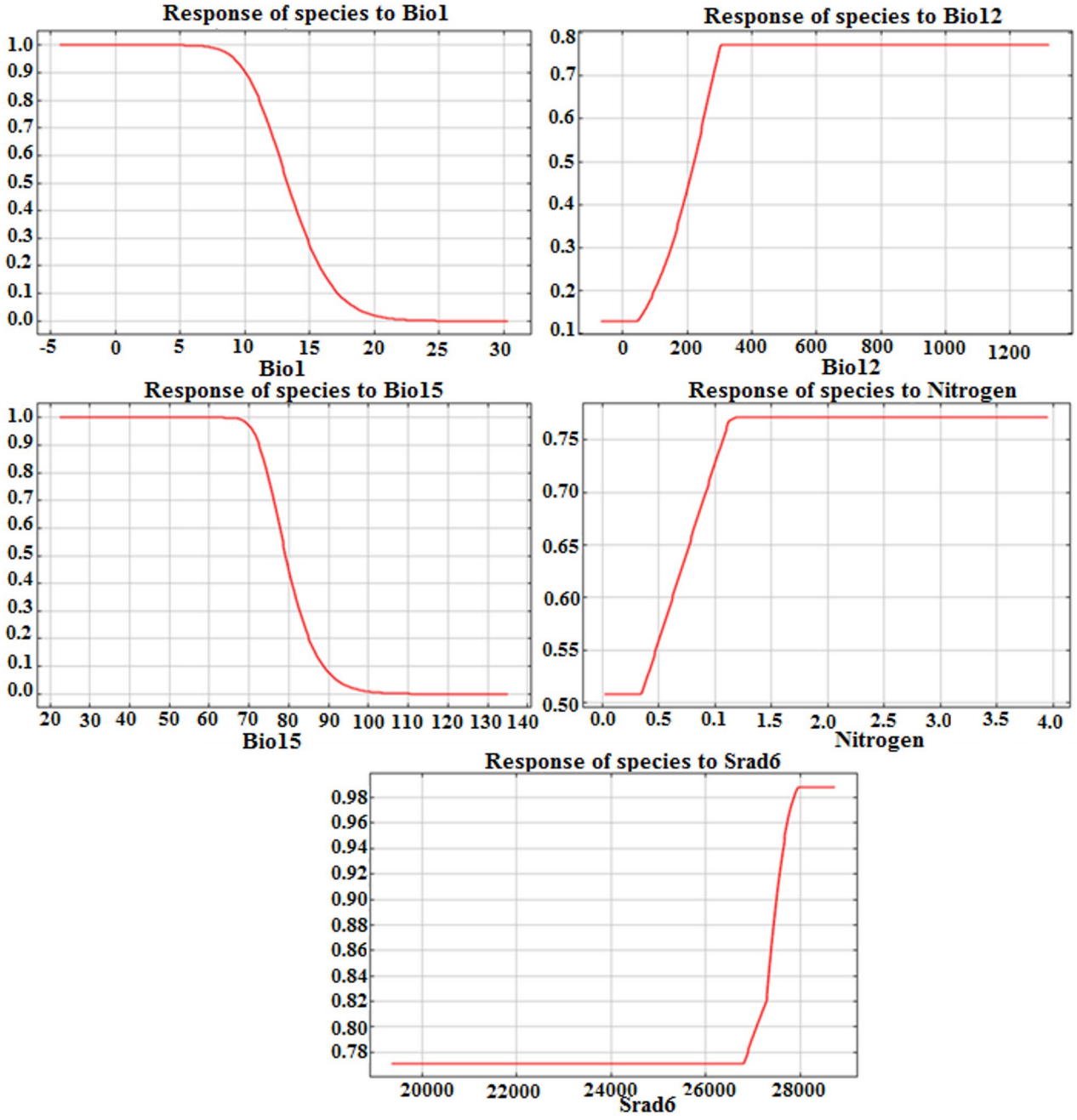

Fig. 6 Response curves of major environmental variables impacting *Salvia multicaulis* under current climate conditions

factors not included in the model, such as dispersal limitations, historical contingencies, land-use patterns, and soil properties [57]. Consequently, the model projects the fundamental niche, whereas the observed distribution represents a subset limited by these unmodeled processes and by the scale of analysis.

Independent spatial prediction maps were generated for each compound and integrated with the habitat suitability layer to produce comprehensive phytochemical quality–suitability maps for *S. multicaulis* (Fig. S3; Fig. 7B). The quantitative analysis reveals a critical distribution across the quality spectrum: a significant portion of the study area, 35,992 km² (25.29%), was classified as having no practical quality (0–0.2.2). Areas of low quality (0.2–0.4) covered 36,984 km² (25.98%), while medium-quality areas (0.4–0.6) accounted for 32,669 km² (22.95%). Most critically, the highest quality class (0.6–1.0.6.0), which signifies the most potent concentrations of medicinally valuable compounds, encompassed 36,687 km² (25.78%) of the region. This high-quality zone was predominantly localized in the western provinces (Hamadan and Kordestan), corresponding to areas of

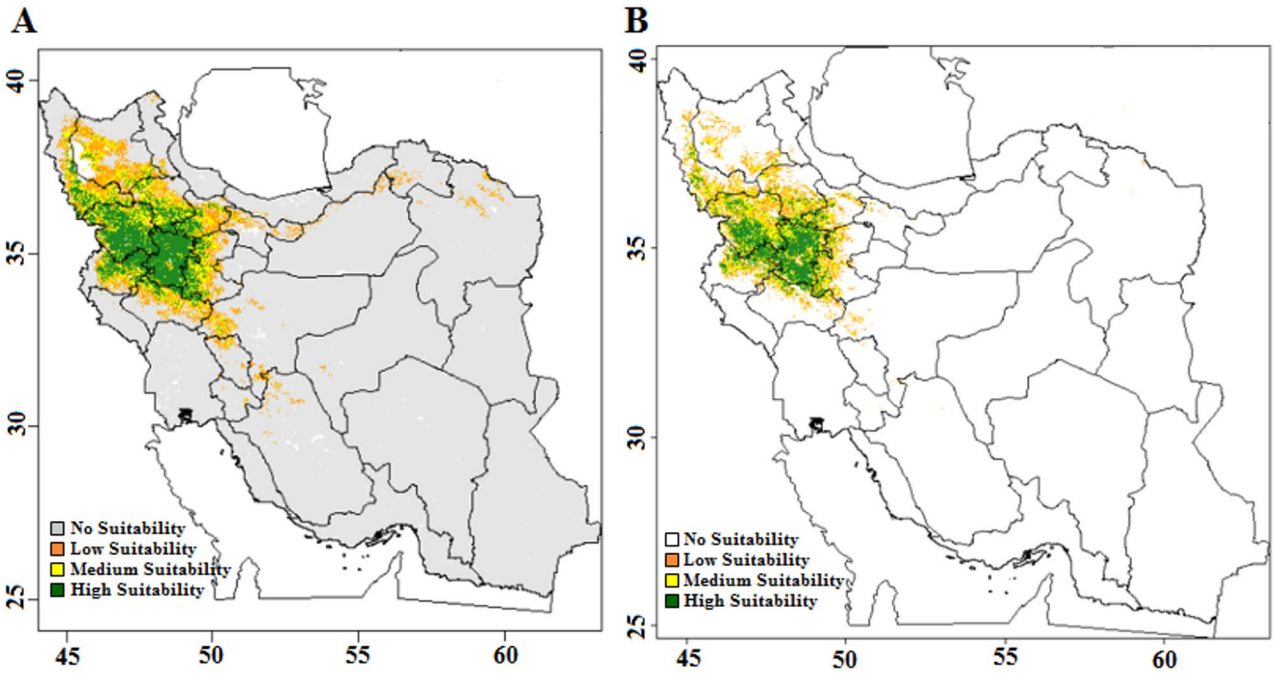

Fig. 7 The zoning map of potential current habitat suitability for Salvia multicaulis (**A**), quality zoning map of S. multicaulis in Iran (**B**). Panels display four suitability classes based on the data-driven classification: No suitability (0–0.2, represented by white or gray), Low suitability (0.2–0.4, orange), Medium suitability (0.4–0.6, yellow), and High suitability (0.6–1, green)

favorable microclimate and edaphic heterogeneity. The near-equal partitioning of the landscape across the four quality classes underscores that the synthesis of bioactive compounds is not uniform but is highly dependent on specific environmental conditions.

A spatial concordance analysis between the habitat suitability map (MaxEnt output) and the integrated phytochemical quality map (RF-based) revealed a strong agreement between the two layers. The overall Cohen's Kappa index was 0.79, indicating substantial consistency, while the agreement in the high suitability–high quality zones was almost perfect (Kappa = 0.86). Notably, 99.5% of the pixels classified as highly suitable also corresponded to areas of high phytochemical quality, highlighting a strong ecological coherence between the modeled habitat suitability and phytochemical accumulation patterns.

Random forest modeling and variable importance for phytochemical composition

The RF models showed moderate but consistent predictive skill across the six phytochemical compounds, with R^2 values ranging from 0.05 (TTC) to 0.54 (TFC), RMSE between 1.26 and 2.63, and MAE between 1.05 and 2.09 (Table S3). Despite the small number of calibration points, these values indicate that the RF algorithm captured a substantial part of the spatial variability in phytochemical quality.

Variable importance analysis revealed distinct environmental controls among compounds (Fig. S2; Table S4). For UA, the most influential predictors were Slope and TRASP; for BA, SOC and Bio14 were dominant. In OA, Slope and Bio14 contributed most, whereas Bio15 and SOC primarily influenced TPC. For TFC, Bio15 and Bio2 emerged as key predictors, while Nitrogen and Srad8 were most important for TTC. The magnitude and direction of %IncMSE values varied across compounds, reflecting differentiated environmental sensitivities of secondary metabolite accumulation.

Future suitable habitats for *S. multicaulis*

The comparison of predicted habitat suitability for *S. multicaulis* under EC-Earth3-Veg and MPI-ESM1-2-HR models across two future periods (2050s and 2070s) and two emission scenarios (SSP245 and SSP585) revealed clear and quantifiable spatial dynamics (Table 2 and Table S4, Figs. 8 and 9). For all scenarios, both gains and losses in suitable areas were recorded, and these changes have been quantified for each model (Table S5-S12).

The EC-Earth3-Veg model consistently projected a net increase in suitable habitat across all timeframes, with future suitable area ranging from 320,478 km^2 (SSP245-2050s, + 3.69%) to 327,528 km^2 (SSP585-2070s, + 5.97%), reflecting a gain that exceeds the concurrent losses in all scenarios (Table 2 and Table S4). Gain areas increased from 54,250 km^2 (SSP245-2050s) to 65,899 km^2 (SSP585-2050s), followed by minor reductions or stabilization

Table 2 The potential distribution area of *Salvia multicaulis* in the 2050 s and 2070s

Species	Models	Period	Area of each suitable region (Km^2)			
S. multicaulis			Unsuitable region	Stable region	Gain region	Loss region
	EC-Earth3-Veg	Present vs. SSP245-2050s	1242361.15	266227.80	54250.48	42842.09
		Present vs. SSP585-2050s	1230712.29	254826.51	65899.35	54243.39
		Present vs. SSP245-2070s	1238572.31	265798.62	58039.32	43271.27
		Present vs. SSP585-2070s	1234706.85	265623.40	61904.78	43446.49
	MPI-ESM1-2-HR	Present vs. SSP245-2050s	1257183.82	242793.86	39427.81	66276.03
		Present vs. SSP585-2050s	1250269.41	262091.35	46342.22	46978.54
		Present vs. SSP245-2070s	1251557.66	255741.62	45053.97	53328.27
		Present vs. SSP585-2070s	1247198.47	267763.62	49413.16	41306.27

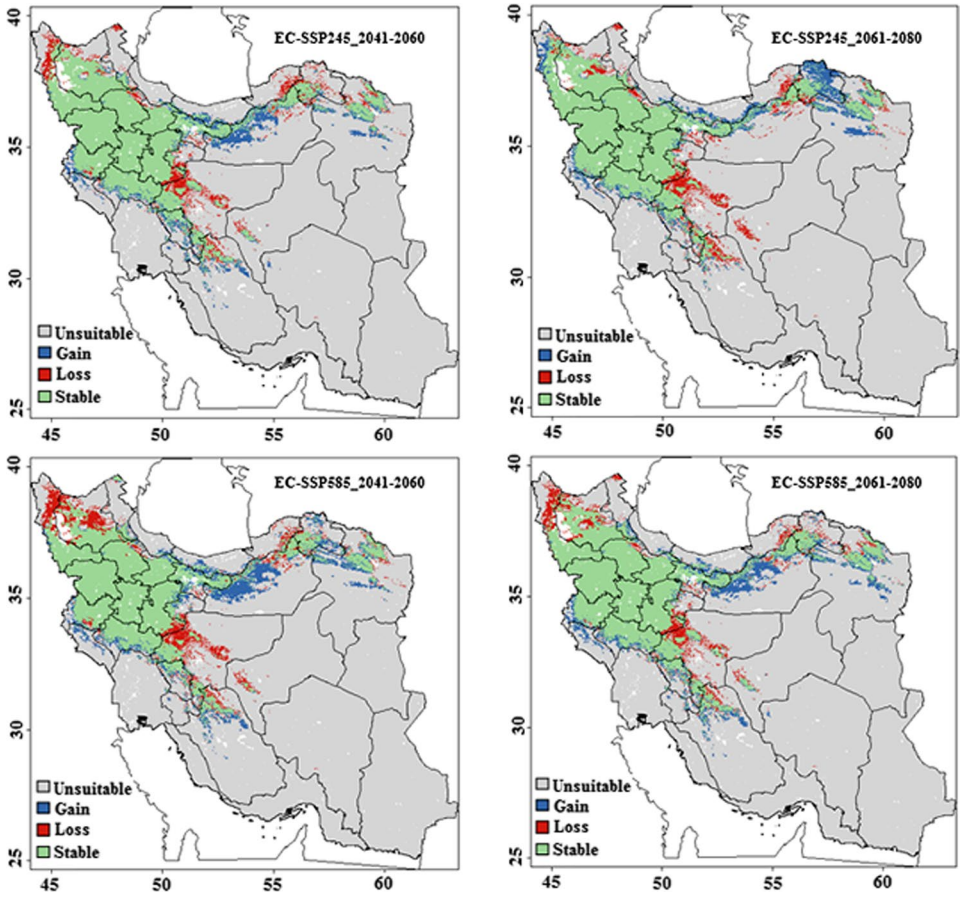

Fig. 8 Suitable habitats for *Salvia multicaulis* under future climate conditions and EC-Earth3-Veg model (EC)

in the 2070s. Conversely, the MPI-ESM1-2-HR model showed smaller and more variable suitable areas, with future suitable area ranging from 282,222 km^2 (SSP245-2050s, – 8.69%) to 317,177 km^2 (SSP585-2070s, + 2.62%), demonstrating that loss areas sometimes exceeded gains.

When averaging the two models, the net projected change in habitat suitability varied from – 2.50% (SSP245-2050s) to + 4.30% (SSP585-2070s), highlighting that *S. multicaulis* is expected to experience moderate stability under most climate scenarios, with potential expansions under higher emission trajectories (SSP585) (Table S5). Environmental drivers such as rising temperature, solar radiation in June, precipitation, and soil nitrogen content were identified as key factors influencing both the formation of new suitable areas and the maintenance of stable habitats.

Across all climate scenarios and models, the area of *S. multicaulis* habitats showed a consistent redistribution among suitability classes rather than a uniform expansion or contraction. Under the SSP245 and SSP585 scenarios for both 2050 s and 2070 s, unsuitable areas are projected to increase by 24,000–87,000 km^2, primarily at the expense of medium and high suitability zones, which are expected to decline by approximately 15,000–26,000 km^2

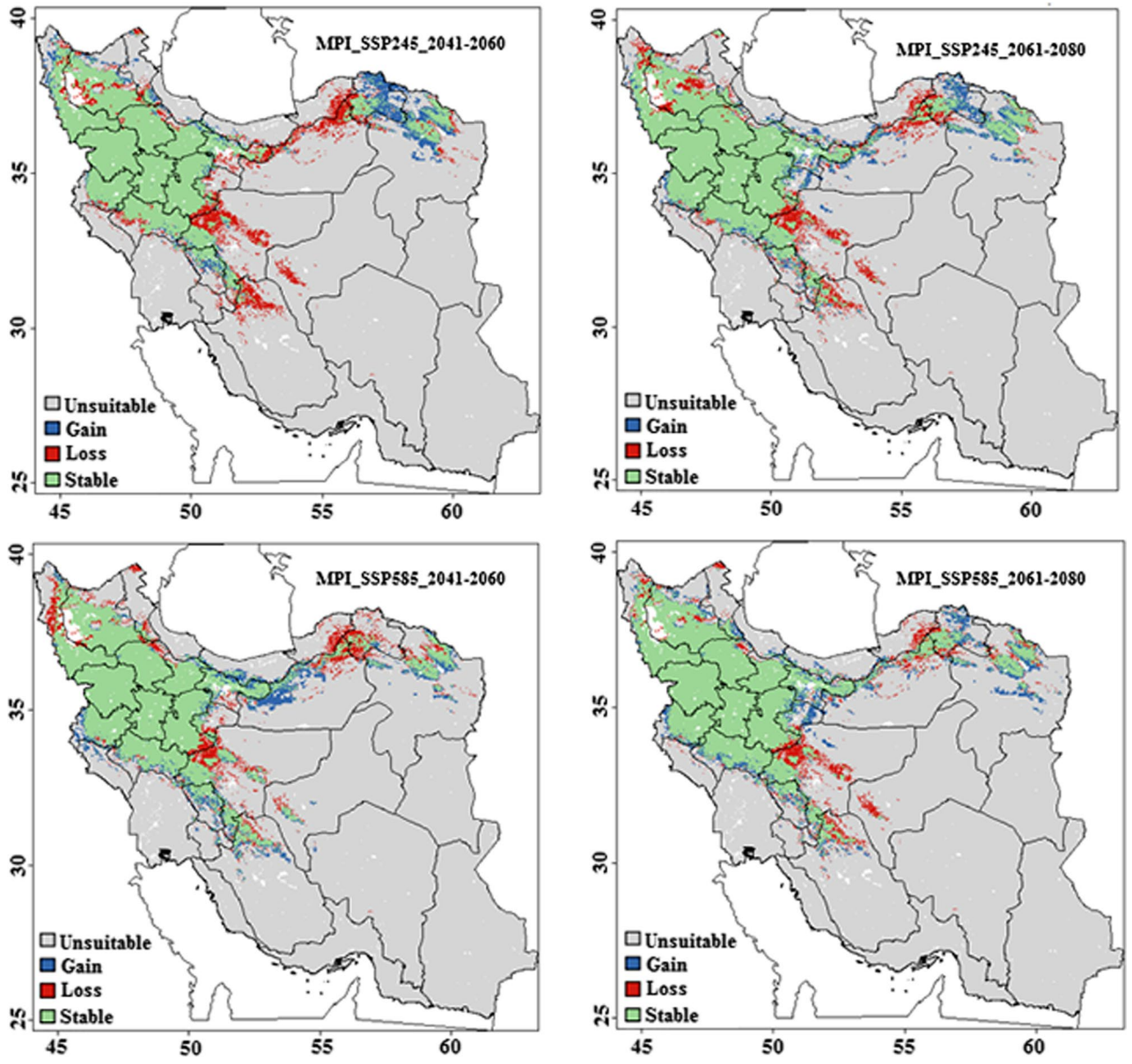

Fig. 9 Suitable habitats for *Salvia multicaulis* under future climate conditions and MPI-ESM1-2-HR model (MPI)

and 10,000–20,000 km², respectively. Low suitability zones exhibited variable patterns, with moderate reductions (–4,000 to – 45,000 km²) depending on the emission pathway and model. Collectively, these patterns indicate a northward and elevational shift of suitable habitats accompanied by fragmentation and degradation of high-quality zones, particularly under the high-emission SSP585 scenario (Table S6-S13).

Furthermore, in terms of quality zoning, the spatial distribution of *S. multicaulis* chemical classes is projected to undergo significant fluctuations under the high-emission SSP585 scenario in both the 2050 s and 2070 s (Table S14-S17). The projections from the EC-Earth3-Veg and MPI-ESM1-2-HR models reveal a consistent trend of a drastic contraction in high-quality areas, with the EC-Earth3-Veg model projecting losses of 43,663 km² by the 2070 s, representing over 97% of current high-quality habitats. This decline is mirrored in the MPI-ESM1-2-HR projections, showing losses of 40,188 km². Concurrently, unsuitable areas expand dramatically, increasing by up to 38,047 km² under EC-Earth3-Veg 2070 s, while low-quality zones show substantial expansion, particularly in MPI-ESM1-2-HR projections (up to 28,703 km²). Meanwhile, the medium-quality class is generally projected to decrease, with the most significant loss (16,117 km²) forecasted by the EC-Earth3-Veg model for the 2070s.

Collectively, these shifts indicate a pronounced redistribution and degradation of chemical quality, suggesting that the proportion of zones sustaining high concentrations of bioactive metabolites is expected to diminish significantly under future climatic stress, while lower-quality and unsuitable habitats expand.

Projections under future climatic scenarios indicate a pronounced decline in phytochemical quality across several regions, most notably within Hamedan and Kurdistan provinces. In contrast, highland zones of Ghazvin, Alborz, Zanjan, West Azerbaijan, Markazi, Lorestan, and Kermanshah are expected to exhibit either stability or moderate improvements in quality (Figs. 10 and 11). Furthermore, newly gained suitable areas are projected in Tehran, East Azerbaijan, Razavi Khorasan, Chaharmahall and Bakhtiari, and Esfahan. Collectively, these regions may function as future refugia, safeguarding the production of high-quality phytochemicals under changing climatic conditions.

Notably, the projected fragmentation and overall contraction of high-quality zones underscore the inherent vulnerability of chemically rich habitats to climate change. This finding highlights the pressing need for proactive conservation strategies, the reassessment of suitable cultivation areas, and the promotion of sustainable harvesting practices from natural populations to ensure long-term resilience under anticipated environmental shifts.

Discussion

Analysis of habitat suitability under the investigated scenarios

Climate change represents a critical driver of ecological shifts that directly affect the survival, spatial distribution, and phytochemical quality of medicinal plants. Variations in the geographic range of these species frequently reflect their adaptive responses to environmental fluctuations, particularly those related to long-term climatic trends. Numerous studies have highlighted that the distribution of medicinal plants is strongly regulated by climatic and topographic variables, with precipitation patterns, temperature gradients, and elevation-related features playing pivotal roles in determining habitat suitability and chemical composition [6, 58].

Under projected future climates, both the EC-Earth3-Veg and MPI-ESM1-2-HR models suggest that *S. multicaulis* will experience moderate spatial shifts in suitable habitat, with the balance between gains, losses, and stable areas varying by emission scenario and model. Quantitative analysis indicates that while EC-Earth3-Veg consistently predicts net habitat gains across all scenarios (up to + 5.97% under SSP585–2070s), MPI-ESM1-2-HR shows a more variable pattern, with net losses occurring under SSP245–2050s (– 8.69%) but moderate gains under SSP585–2070s (+ 2.62%). This variability is a common challenge in ecological forecasting, with systematic reviews confirming that regional projections of global

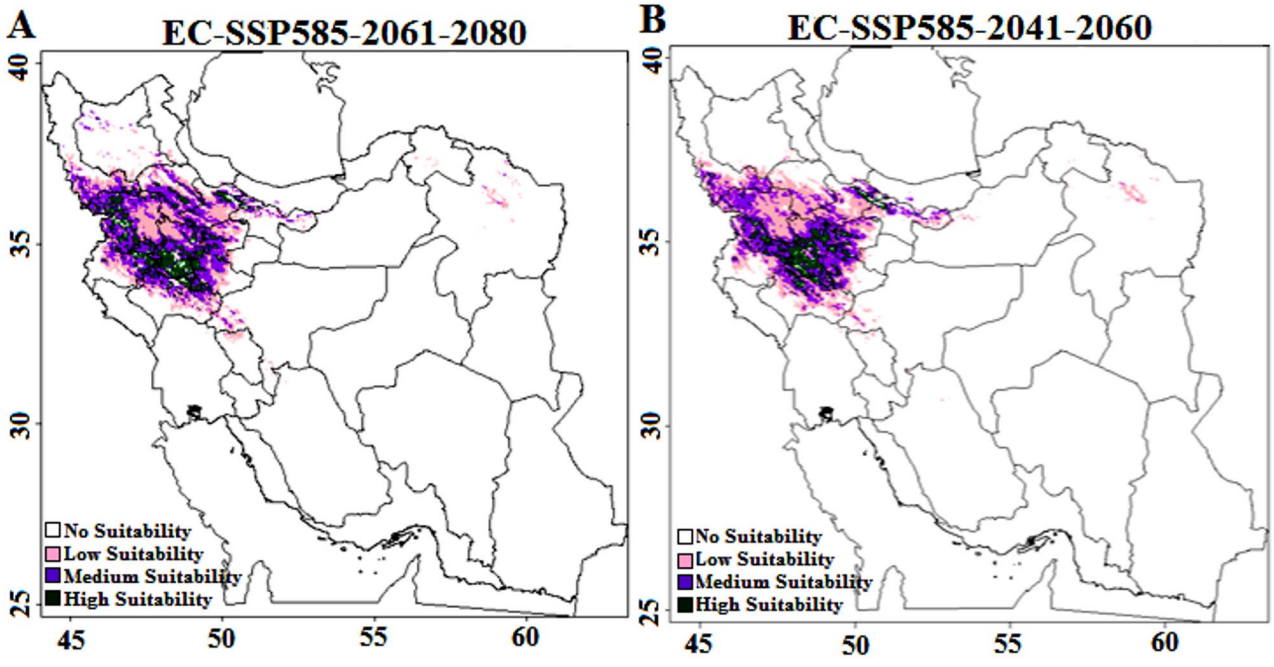

Fig. 10 The quality zoning maps of *Salvia multicaulis* in Iran under EC-Earth3-Veg model and the SSP585 scenario for 2050 (2041–2060) and 2070 (2061 – 280)The quality zoning maps of Salvia multicaulis in Iran under EC-Earth3-Veg model and the SSP585 scenario for 2050 (2041-2060) and 2070 (2061-280). Panels display four suitability classes based on the data-driven classification: No suitability (0–0.2, represented by white), Low suitability (0.2–0.4, pink), Medium suitability (0.4–0.6, dark purple), and High suitability (0.6–1, green)

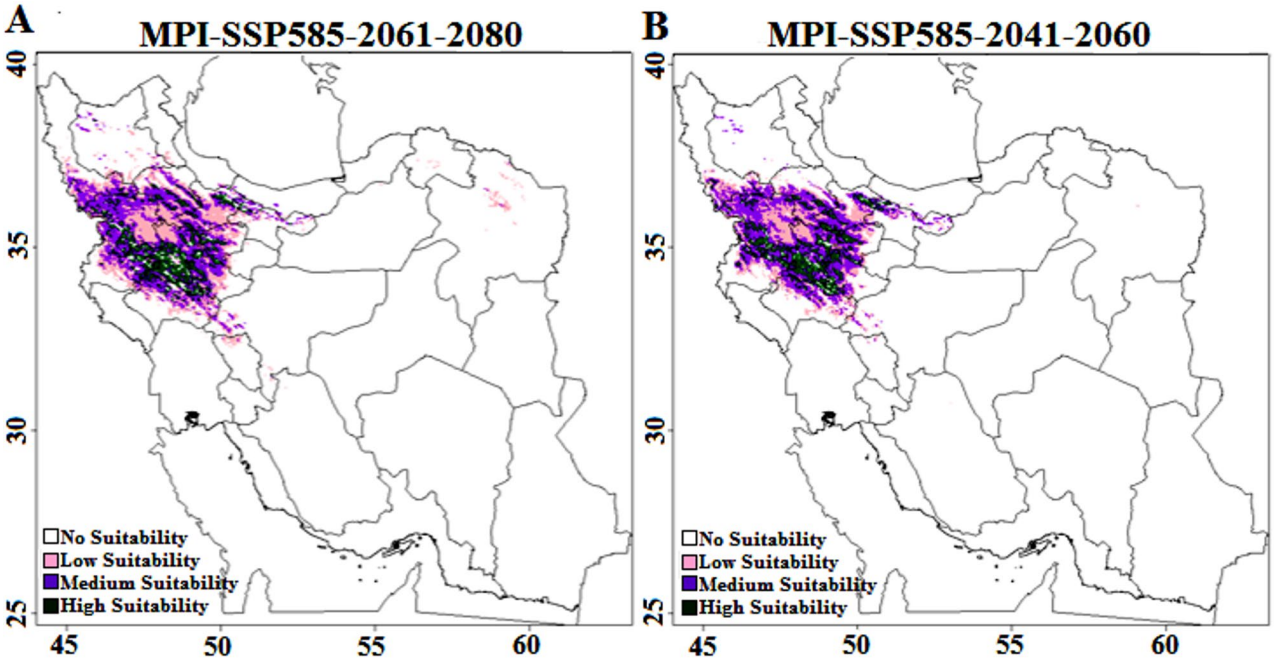

Fig. 11 The quality zoning maps of Salvia multicaulis in Iran under MPI-ESM1-2-HR model and the SSP585 scenario for 2050 (2041-2060) and 2070 (2061-280). Panels display four suitability classes based on the data-driven classification: No suitability (0–0.2, represented by white), Low suitability (0.2–0.4, pink), Medium suitability (0.4–0.6, dark purple), and High suitability (0.6–1, green)

scenarios are often dominated by top-down approaches and can yield a diverse range of outcomes [59]. Our approach, which uses multiple GCMs, is therefore crucial to capture the uncertainty in future climate impacts.

The contrasting outcomes between SSP245 and SSP585 scenarios reflect the complex interplay between species-specific ecological requirements and the magnitude of climate change. Under the moderate SSP245 scenario, subtle shifts in temperature and precipitation may not sufficiently match the species' optimal niche, resulting in contraction of suitable areas, particularly in peripheral regions. Conversely, the more extreme SSP585 scenario appears to generate environmental conditions, such as higher temperatures, increased solar radiation, and potentially more favorable soil nutrients, that align with the ecological preferences of *S. multicaulis* in certain regions, enabling expansion. This seemingly counterintuitive result, where a high-emission scenario facilitates range expansion, finds parallels in other studies. For instance, a projection study for five Brazilian plant species found that *Qualea multiflora* could gain up to 92.21% in new suitable areas under future climate scenarios, demonstrating that significant range expansion is a possible response for some species [60]. This supports the notion that combined environmental drivers, rather than temperature alone, govern habitat suitability and that species-level plasticity may allow persistence under broader climatic conditions than current distributions suggest [61].

Although the projected range expansions under SSP585 indicate potential resilience, a nuanced analysis reveals significant conservation challenges. The quantitative data show that gain areas are often smaller and more fragmented than stable zones, implying that new suitable habitats may not fully offset losses, particularly in the vulnerable peripheral regions where loss outweighs gain. This pattern of fragmented gains and geographically shifted habitats is strongly reinforced by observations in other medicinal species. For instance, a study on *Lonicera japonica* Flos similarly projected a northwestward range shift in China, with future suitable habitats becoming increasingly fragmented, directly mirroring our findings for *S. multicaulis* [1]. Furthermore, research on *Illicium verum* Hook. f. (star anise) confirms that while climate change may open new suitable areas, these are often disjunct and subject to ecological bottlenecks, underscoring that potential expansion does not equate to seamless population establishment [53]. The projected spatial shift of suitable habitats towards central, northeastern, and southwestern provinces (e.g., Semnan, North Khorasan, Fars) suggests a potential for range expansion into regions that may retain crucial ecological requirements, such as cold winter temperatures for breaking seed dormancy [53, 62]. However, these potential gains are often fragmented. Therefore, such patterns emphasize the need for proactive conservation strategies, including habitat connectivity and protection of core areas, to facilitate species migration and long-term persistence under

climate change, a critical recommendation for managers planning for species redistribution [63].

Furthermore, beyond climate-driven shifts, the species faces significant anthropogenic pressures in its core and potential future habitats. Unsustainable harvesting for medicinal use and livestock grazing is documented threats that could compound the vulnerability of populations, particularly in fragmented or declining habitats [64]. Therefore, effective conservation plans must integrate measures to mitigate these direct human impacts alongside strategies for climate adaptation.

Analysis of chemical quality within different habitat classes

In the present study, spatial distribution maps of key bioactive compounds—UA, BA, OA, TPC, TFC, and TTC—were integrated with the habitat suitability map to generate a comprehensive quality zoning map of *S. multicaulis* across Iran. The highest-quality populations were predominantly located in the western and northwestern provinces. This geographical pattern can be explained by the optimal range of critical environmental factors found in these regions. Specifically, the moderate climatic conditions, characterized by cooler annual temperatures (Bio1), sufficient but not excessive precipitation (Bio12), along with mild soil nutrients (Nitrogen and SOC) and high light irradiation in the west and northwest, create an ecophysiological niche that is highly conducive for the production of high levels of bioactive compounds in *S. multicaulis* [65, 66]. These findings align with established ecological principles and previous studies on medicinal plants, which consistently highlight the regulatory function of climatic and edaphic factors in defining species quality [1, 4, 53].

The projected spatial redistribution of *S. multicaulis* chemical classes under the high-emission SSP585 scenario points not merely to a geographical shift, but to a profound and concerning qualitative degradation of its medicinal value. The consistent and drastic contraction of high-quality areas coupled with the concurrent expansion of low-quality and unsuitable habitats, signals a potential depletion of populations rich in bioactive metabolites. The expansion of the low-quality class, particularly in the MPI-ESM1-2-HR projections, indicates that many regions may become sub-optimal, supporting survival but not high chemical expression. This pattern of qualitative decline under climate change finds strong parallels in other medicinal species modeled using similar integrated approaches. For instance, a study on *Astragalus membranaceus* var. *mongholicus* (Bunge) P.K. Hsiao demonstrated that future climate change could significantly reduce the geographic area suitable for high-quality roots, directly linking specific environmental stressors to a decrease in the concentration of key bioactive compounds [6]. Similarly, an integrated assessment of *Notopterygium franchetii* H. de Boiss projected that while the overall habitat might persist in some regions, the combined pressure of shifting temperatures and precipitation patterns would lead to a marked decline in medicinal quality, even in parts of its future range [4]. The consistency of this finding across studies underscores that climate change impacts on medicinal plants are twofold: affecting not only where a species can survive but, more critically, the pharmacological potency it can maintain [67]. The drastic conversion of high-quality zones to lower-quality classes in our projections suggests that the environmental optima for the biosynthesis of valuable metabolites like ursolic acid and total phenolics are being severely disrupted. Consequently, conservation strategies must prioritize the protection of current high-quality chemotypes, as the future climate may not support the re-establishment of populations with equivalent medicinal value.

Our comparative analysis of different climate models (EC-Earth3-Veg and MPI-ESM1-2-HR) revealed that the magnitude of these projected shifts in phytochemical quality is sensitive to the choice of climate model, highlighting this as an important source of uncertainty in forecasting future medicinal plant quality. This uncertainty underscores the critical need to understand the fundamental relationship between habitat suitability and phytochemical accumulation.

Relationship between habitat suitability and chemical quality

The strong spatial agreement between the modeled habitat suitability and phytochemical quality layers (Kappa = 0.79 overall; 0.86 for high-quality zones) suggests that the environmental factors driving species distribution are also key determinants of phytochemical accumulation in *S. multicaulis*. This coherence supports the ecological basis of secondary metabolite variation, as both processes are influenced by similar climatic and edaphic gradients such as temperature, moisture, and soil organic carbon. Similar spatial overlaps between suitability and chemical richness have been reported for other medicinal plants, emphasizing that high-quality habitats often coincide with ecologically optimal niches [1, 4].

Furthermore, the overlap between low-quality medicinal zones and unsuitable habitats suggests that adverse environmental conditions not only hinder the growth of *S. multicaulis* but also limit the accumulation of its key secondary metabolites. However, it is important to recognize that habitat suitability does not always guarantee high phytochemical quality. The biosynthesis of secondary metabolites is tightly regulated by complex plant physiological and biochemical responses, which are shaped by both genetic potential and environmental cues [68]. While favorable conditions support biomass

production, moderate abiotic stresses, such as drought, temperature fluctuations, or nutrient limitations, can act as triggers for enhanced metabolite synthesis [65, 68].

This dual dependence suggests that "quality refugia", areas maintaining both ecological suitability and moderate environmental stress, may represent priority conservation targets, as they sustain both population viability and high phytochemical potential [66]. Therefore, under future climate scenarios, conservation and cultivation strategies should prioritize areas where favorable soil characteristics (e.g., high SOC and nitrogen) co-occur with topoclimatic features that sustain the species' chemical potential.

The identification and protection of such zones will be essential to safeguarding both ecological viability and the pharmaceutical value of *S. multicaulis* in the face of accelerating climate change. These findings are consistent with previous studies reporting that spatial and temporal variations in environmental conditions, such as temperature, precipitation, solar radiation, and soil properties, can significantly influence the accumulation and composition of plant secondary metabolites across different geographic regions [1, 6, 69, 70].

Study limitations and future research directions

While this study provides comprehensive insights into the eco-phytochemical dynamics of *S. multicaulis*, certain limitations should be acknowledged. The primary constraint is the sample size of 17 populations, which, while geographically diverse, may not capture the full chemotypic diversity present across the species' entire ecological range. Furthermore, the projections of future chemical quality are contingent upon the uncertainties inherent in the underlying global climate models and emission scenarios. Future research should prioritize expanding the sampling framework to encompass a broader genetic and environmental gradient. Integrating genomic tools to elucidate the genetic basis of chemotypic variation would significantly enhance our mechanistic understanding. Finally, developing habitat suitability models that incorporate key biotic interactions and direct anthropogenic pressures, such as targeted harvesting, would yield a more holistic forecasting framework for conservation planning.

Conclusion

The present study provides an integrated assessment of the habitat suitability and phytochemical quality of *S. multicaulis* under current and future climate scenarios. Our findings demonstrate that the species' distribution and its accumulation of bioactive compounds are predominantly governed by a suite of climatic and edaphic factors, with annual mean temperature (Bio1), annual precipitation (Bio12), soil nitrogen, and solar radiation (Srad6) identified as the key environmental drivers. Chemometric analysis confirmed distinct spatial chemotypes, correlating with these ecological gradients. Future projections under the high-emission SSP5-8.5 scenario reveal a concerning trajectory not of a simple geographical shift, but of a profound qualitative degradation. We project a severe contraction of high-quality habitats, with losses exceeding 42,000 km², alongside a significant expansion of unsuitable and low-quality areas. This underscores a direct threat to the species' medicinal value. The strong spatial agreement between modeled habitat suitability and phytochemical quality (Kappa = 0.79) confirms that the environmental factors defining the species' niche are also crucial determinants of its pharmaceutical potential. Consequently, "quality refugia", areas that maintain ecological suitability under future climates, must be prioritized for conservation. This research underscores the critical need for conservation strategies that move beyond safeguarding mere presence to actively preserving pharmacological value. We recommend targeted protection of identified high-quality chemotypes, sustainable harvesting practices, and the assisted migration or cultivation of valuable populations into future climatically resilient zones to ensure the long-term ecological and medicinal sustainability of *S. multicaulis*.

Supplementary Information

The online version contains supplementary material available at https://doi.org/10.1186/s12870-025-07756-4.

Supplementary Material 1.

Acknowledgements

The authors thank Bu Ali Sina University, Hamedan, Iran for their financial support.

Identification of the collected plant materials

The identification and authentication of Salvia multicaulis as a species was done by Dr. Ranjbar and vouchered in Bu Ali Sina University Herbarium (Number: A-Hort-97-SMP).

Authors' contributions

M.T.: Writing – review & editing, Writing – original draft, Visualization, Methodology, Conceptualization. **A.A.:** Writing – review & editing, Supervision, Project administration, Methodology, Conceptualization. **H.S.:** Writing – review & editing, Methodology, Conceptualization. **E.D.:** Writing – review & editing, Methodology, Conceptualization. **M.M.R.:** Writing – review & editing, Methodology, Conceptualization. **M.H.M.:** Writing – review & editing, Supervision, Methodology, Conceptualization.

Funding

Not applicable.

Data availability

Data will be made available on request.

Declarations

Ethics approval and consent to participate

All methods performed in this study were in compliance with the relevant institutional, national, and international guidelines and legislation.

Consent for publication
Not applicable.

Competing interests
The authors declare no competing interests.

Received: 30 August 2025 / Accepted: 13 November 2025
Published online: 06 December 2025

References

1. Cheng J, Guo F, Wang L, Li Z, Zhou C, Wang H, et al. Evaluating the impact of ecological factors on the quality and habitat distribution of *Lonicera Japonica* Flos using HPLC and the maxent model. Front Plant Sci. 2024;15:1–15. https://doi.org/10.3389/fpls.2024.1397939.
2. Davis CC, Choisy P. Medicinal plants Meet modern biodiversity science. Curr Biol Cell Press. 2024;34:R158–73. https://doi.org/10.1016/j.cub.2023.12.038.
3. Yang L, Miao L, Gong Q, et al. Advances in studies on transcription factors in regulation of secondary metabolites in Chinese medicinal plants. Plant Cell Tiss Organ Cult. 2022;151:1–9. https://doi.org/10.1007/s11240-022-02334-0.
4. Wan G, Li Q, Jin L, Chen J. Integrated approach to predicting habitat suitability and evaluating quality variations of *Notopterygium Franchetii* under climate change. Sci Rep. 2024;14:26927. https://doi.org/10.1038/s41598-024-77824-6.
5. Wu Z, Ye X, Bian F, Yu G, Gao G, Ou J, et al. Determination of the geographical origin of *Tetrastigma Hemsleyanum* diels & Gilg using an electronic nose technique with multiple algorithms. Heliyon. 2022;8:e10801. https://doi.org/10.1016/j.heliyon.2022.e10801.
6. Dong P, Wang L, Qiu D, Liang W, Cheng J, Wang H et al. Evaluation of the environmental factors influencing the quality of *Astragalus membranaceus var. mongholicus* based on HPLC and the Maxent model. BMC Plant Biol. 2024;24:697. https://doi.org/10.1186/s12870-024-05355-3
7. Huang Z, Xie L, Wang H, Zhong J, Li Y, Liu J, et al. Geographic distribution and impacts of climate change on the suitable habitats of *Zingiber* species in China. Ind Crop Prod. 2019;138:111429. https://doi.org/10.1016/j.indcrop.2019.05.078.
8. Chandora R, Paul S, Kumar P, Singh B, Kumar P, Sharma A, et al. Ecological survey, population assessment and habitat distribution modelling for conserving *Fritillaria roylei*—A critically endangered Himalayan medicinal herb. South Afr J Bot. 2023;160:75–87. https://doi.org/10.1016/j.sajb.2023.06.057.
9. Suppula M, Hällfors MH, Aapala K, Aalto J, Kemppainen E, Leikola N, et al. Climate and land-use change drive population decline in a red-listed plant species. Glob Ecol Conserv. 2023;45:e02526. https://doi.org/10.1016/j.gecco.2023.e02526.
10. Hojati M, Naderi R, Edalat M, Pourghasemi HR. Modelling key ecological factors influencing the distribution and content of Silymarin antioxidant in *Silybum Marianum* L. PLoS ONE. 2025;20:e0322442. https://doi.org/10.1371/journal.pone.0322442.
11. Phillips SJ, Dudík M, Elith J, Graham CH, Lehmann A, Leathwick J, et al. Sample selection bias and presence-only distribution models: implications for background and pseudo-absence data. Ecol Appl. 2009;19:181–97. https://doi.org/10.1890/07-2153.1.
12. Khan AM, Li Q, Saqib Z, Khan N, Habib T, Khalid N. MaxEnt modelling and impact of climate change on habitat suitability variations of economically important Chilgoza pine (*Pinus Gerardiana* Wall.) in South Asia. Forests. 2022;13:715. https://doi.org/10.3390/f13050715.
13. Ahmadi M, Hemami MR, Kaboli M, Shabani F. MaxEnt brings comparable results when the input data are being completed; model parameterization of four species distribution models. Ecol Evol. 2023;13:e9827. https://doi.org/10.1002/ece3.9827.
14. Elith J, Leathwick JR. Species distribution models: ecological explanation and prediction across space and time. Annu Rev Ecol Evol Syst. 2009;40:677–97.
15. Koch R, Almeida-Cortez JS, Kleinschmit B. Revealing areas of high nature conservation importance in a seasonally dry tropical forest in brazil: combination of modelled plant diversity hot spots and threat patterns. J Nat Conserv. 2017;35:24–39. https://doi.org/10.1016/j.jnc.2016.11.004.
16. Zeng J, Li C, Liu J, Li Y, Hu Z, et al. Ecological assessment of current and future *Pogostemon Cablin* Benth. Potential planting regions in China based on maxent and ArcGIS models. J Appl Res Med Aromat Plants. 2021;24:100308. https://doi.org/10.1016/j.jarmap.2021.100308.
17. Elith J, Phillips SJ, Hastie T, Dudík M, Chee YE, Yates CJ. A statistical explanation of maxent for ecologists. Divers Distrib. 2011;17:43–57.
18. Phillips SB, Aneja VP, Kang D, Arya SP. Modelling and analysis of the atmospheric nitrogen deposition in North Carolina. Int J Glob Environ Issues. 2006;6:231–52.
19. Riahi K, van Vuuren DP, Kriegler E, Edmonds J, O'Neill BC, Fujimori S, et al. The shared socioeconomic pathways and their energy, land use, and greenhouse gas emissions implications: an overview. Glob Environ Chang. 2017;42:153–68.
20. IPCC. Climate change 2021: The physical science BaIPCC. (2021). Climate change 2021: The physical science basis: summary for policymakers technical summary frequently asked questions glossary. In Intergovernmental Panel on Climate Change. www.ipcc.chsis: Summar. Intergov. Panel Clim. Chang. 2021.
21. O'Neill BC, Kriegler E, Riahi K, Ebi KL, Hallegatte S, Carter TR, et al. A new scenario framework for climate change research: the concept of shared socioeconomic pathways. Clim Change. 2014;122:387–400. https://doi.org/10.1007/s10584-013-0905-2.
22. Kaky E, Nolan V, Alatawi A, Gilbert F. A comparison between ensemble and maxent species distribution modelling approaches for conservation: A case study with Egyptian medicinal plants. Ecol Inf. 2020;60:101150. https://doi.org/10.1016/j.ecoinf.2020.101150.
23. Lee WH, Song JW, Yoon SH, Jung JM. Spatial evaluation of machine learning-based species distribution models for prediction of invasive ant species distribution. Appl Sci. 2022;12:10260. https://doi.org/10.3390/app122010260.
24. Wu F, Wang Y, Zheng M, Wang J, Pan J, Liu L. Prediction and quality zoning of potentially suitable areas for *Panax Notoginseng* cultivation using maxent and random forest algorithms in Yunnan Province, China. Ind Crops Prod. 2025;229:120960. https://doi.org/10.1016/j.indcrop.2025.120960.
25. Abolmaali SMR, Tarkesh M, Bashari H. MaxEnt modeling for predicting suitable habitats and identifying the effects of climate change on a threatened species, *Daphne mucronata*, in central Iran. Ecol Inf. 2018;43:116–23. https://doi.org/10.1016/j.ecoinf.2017.10.002.
26. Zare M, Moameri M, Ghorbani A, Sahragard HP, Mostafazadeh R, Dadjou F, et al. Modeling habitat suitability of *Dorema ammoniacum* D Don. In the rangelands of central Iran. Sci Rep. 2024;14:1–14. https://doi.org/10.1038/s41598-024-61073-8.
27. Noedoost F, Behroozian M, Karami S, Joharchi MR. Potential impacts of climate change on the geographic distribution of *Achillea eriophora* DC., a medicinal species endemic to Iran in Southwestern Asia. Ecol Evol. 2024;14:1–12.
28. Hosseini N, Ghorbanpour M, Mostafavi H. The influence of climate change on the future distribution of two *Thymus species* in iran: maxent model-based prediction. BMC Plant Biol. 2024;24:1–14.
29. Ulubelen A, Topcu G. Chemical and biological investigations of *Salvia* species growing in Turkey. 1997;20:659–718. https://doi.org/10.1016/S1572-5995(97)80040-3
30. Tavan M, Azizi A, Sarikhani H, Mirjalili MH, Rigano MM. Phenolics diversity among wild populations of *Salvia multicaulis*: as a precious source for antimicrobial and antioxidant applications. Nat Prod Res. 2022;36:1332–6. https://doi.org/10.1080/14786419.2020.1864369.
31. Barhoumi LM, Al-Jaber HI, Abu Zarga MH. A new diterpene and other constituents of *Salvia multicaulis* from Jordan. Nat Prod Res. 2022;36:4921–8. https://doi.org/10.1080/14786419.2021.1912745.
32. Tavan M, Azizi A, Sarikhani H, Mirjalili MH, Rigano MM. Induced polyploidy and broad variation in phytochemical traits and altered gene expression in *Salvia multicaulis*. Sci Hortic. 2022;291:110592. https://doi.org/10.1016/j.scienta.2021.110592.
33. Pehlivan M, Sevindik M. Antioxidant and antimicrobial activities of *Salvia multicaulis*. TURJAF. 2018;6:628–31. https://doi.org/10.24925/turjaf.v6i5.628-631.1906.
34. Abdallah Q, Al-Deeb I, Bader A, Hamam F, Saleh K, Abdulmajid A. Anti-angiogenic activity of middle East medicinal plants of the lamiaceae family. Mol Med Rep. 2018;18:2441–8. https://doi.org/10.3892/mmr.2018.9155.
35. Rechinger KH. Labiatae – Flora Iranica 150. Rechinger KH. editor. Graz, Austria: Akademische Druck- u. Verlagsanstalt; 1982.
36. Mohammadhosseini M, Pazoki A, Akhlaghi H. Chemical composition of the essential oils from flowers, leaves, stems and roots of *Hypericum perforatum* L. from Iran. Chem Nat Compd. 2008;44:127–8.
37. Jahromi MS, Azizi A, Soltani J. Diversity and Spatiotemporal distribution of fungal endophytes associated with *Salvia multicaulis*. Curr Microbiol. 2021;78:1432–47. https://doi.org/10.1007/s00284-021-02430-y.

38. Tavakoli M, Tarkesh Esfahani M, Soltani S, Karamian R, Aliarabi H. Effects of ecological factors on phenolic compounds in *Salvia multicaulis* Vahl (Lamiaceae). Biochem Syst Ecol. 2022;104:104484. https://doi.org/10.1016/j.bse.2022.104484.
39. Sagheb Talebi K, Sajedi T, Pourhashemi M. Forests of Iran. Springer Dordrecht; 2014.
40. Najafi MS, Alizadeh O. Climate zones in Iran. Meteorol Appl. 2023;30:1–10.
41. Talebi SM, Askary M, Khalili N, Matsyura A, Ghorbanpour M, Kariman K. Genetic structure and essential oil composition in wild populations of *Salvia multicaulis* Vahl. Biochem Syst Ecol. 2021;96:104269. https://doi.org/10.1016/j.bse.2021.104269.
42. Ainsworth EA, Gillespie KM. Estimation of total phenolic content and other oxidation substrates in plant tissues using Folin-Ciocalteu reagent. Nat Protoc. 2007;2:875–7. https://doi.org/10.1038/nprot.2007.102.
43. Kamtekar S, Keer V, Patil V. Estimation of phenolic content, flavonoid content, antioxidant and alpha amylase inhibitory activity of marketed polyherbal formulation. J Appl Pharm Sci. 2014;4:61–5. https://doi.org/10.7324/JAPS.2014.40911.
44. Galvão MA, Arruda AO, Bezerra IC, Ferreira MR, Soares LA. Evaluation of the Folin-Ciocalteu method and quantification of total tannins in stem barks and pods from *Libidibia Ferrea* (Mart. Ex Tul) LP Queiroz. Braz Arch Biol Technol. 2018;61:e18170586. https://doi.org/10.1590/1678-4324-2018170586.
45. Cohen J. Statistical power analysis for the behavioral sciences (2nd ed.). Hillsdale NLEA, editor. 1988.
46. Kamangar M, Ahmadi M, Rabiei-Dastjerdi H, Hazbavi Z. Ensemble modeling of extreme seasonal temperature trends in Iran under socio-economic scenarios. Nat Hazards. 2025;121:1265–88.
47. Zabihi O, Ahmadi A. Multi-criteria evaluation of CMIP6 precipitation and temperature simulations over Iran. J Hydrol Reg Stud. 2024;52:101707. https://doi.org/10.1016/j.ejrh.2024.101707.
48. Hosseinpour S, Sharafati A, Abghari H. Evaluation of general circulation models in simulating Spatial patterns of climate variables over various regions of Iran. J Water Clim Chang. 2025;16:1782–803.
49. Azad N, Ahmadi A. Assessment of CMIP6 models and multi-model averaging for temperature and precipitation over Iran. Sci Rep. 2024;14:1–19.
50. Hair JF, Black WC, Babin BJ, Anderson RE. Multivariate data analysis. 7th Edition, Pearson,. New York.; 2010.
51. Neter J, Kutner MH, Nachtsheim CJ, Wasserman W. Applied linear statistical models. 4th Edition,. WCB McGraw-Hill, New York.; 1996.
52. Valavi R, Guillera-Arroita G, Lahoz-Monfort JJ, Elith J. Predictive performance of presence-only species distribution models: a benchmark study with reproducible code. Ecol Monogr. 2022;92:1–27.
53. Gu P, Li Q, Li L, Huang D, Cao K, Lu R, et al. Habitat suitability assessment for *Illicium verum* Hook. f. (Star Anise) under climate change conditions, using the maxent model and comprehensive 2D chromatography. Agronomy. 2024;14:2858. https://doi.org/10.3390/agronomy14122858.
54. Jenks GF. The data model concept in statistical mapping. International Yearbook of Cartography; 1967.
55. Zheng T, Sun J, qian, Shi X jun, Liu D, ling, Sun B yin, Deng Y et al. Evaluation of climate factors affecting the quality of red huajiao (*Zanthoxylum bungeanum* maxim.) based on UPLC-MS/MS and MaxEnt model. Food Chem X. 2022;16:100522. https://doi.org/10.1016/j.fochx.2022.100522
56. Zhang H, Yang S, Wei X, Wang L, Sun X, Hou Z, et al. Forecasting the favorable growth conditions and suitable regions for Chicory (*Cichorium intybus* L.) on the *Qinghai plateau* under current Climatic conditions. Ecol Inf. 2023;78:102343. https://doi.org/10.1016/j.ecoinf.2023.102343.
57. Guisan A, Thuiller W. Predicting species distribution: offering more than simple habitat models. Ecol Lett. 2005;8:993–1009.
58. Kumar S, Spaulding SA, Stohlgren TJ, Hermann KA, Schmidt TS, Bahls LL. Potential habitat distribution for the freshwater diatom *Didymosphenia geminata* in the continental US. Front Ecol Environ. 2009;7:415–20. https://doi.org/10.1890/080054.
59. Pedde S, Kok K, Kemp-Benedict E, Johnson O, Carlsen H, Green C, et al. Emerging regional perspectives of global climate change scenarios: a systematic review. Clim Change. 2025;178:1–19.
60. Alves-de-Lima L, Alves DFR, Anjos DV, Valdivia FA, Torezan-Silingardi HM. Predicting the impact of global climate change on the geographic distribution of anemochoric species in protected areas. Atmos (Basel). 2025;16:453. https://doi.org/10.3390/atmos16040453.
61. Nicotra AB, Atkin OK, Bonser SP, Davidson AM, Finnegan EJ, Mathesius U, et al. Plant phenotypic plasticity in a changing climate. Trends Plant Sci. 2010;15:684–92. https://doi.org/10.1016/j.tplants.2010.09.008.
62. Nuñez TA, Prugh LR, Lambers JHR. Animal-mediated plant niche tracking in a changing climate. Trends Ecol Evol. 2023;38:654–65.
63. Rubenstein MA, Weiskopf SR, Bertrand R, Carter SL, Comte L, Eaton MJ, et al. Climate change and the global redistribution of biodiversity: substantial variation in empirical support for expected range shifts. Environ Evid. 2023;12:1–21. https://doi.org/10.1186/s13750-023-00296-0.
64. Chapagain DJ, Meilby H, Baniya CB, Budha-Magar S, Ghimire SK. Illegal harvesting and livestock grazing threaten the endangered Orchid *Dactylorhiza Hatagirea* (D. Don) Soó in Nepalese himalaya. Ecol Evol. 2021;11:6672–87.
65. Yang L, Wen KS, Ruan X, Zhao YX, Wei F, Wang Q. Response of plant secondary metabolites to environmental factors. Molecules. 2018;23:1–26.
66. Jangpangi D, Patni B, Chandola V, Chandra S. Medicinal plants in a changing climate: Understanding the links between environmental stress and secondary metabolite synthesis. Front Plant Sci. 2025;16:1–15.
67. Shen T, Yu H, Wang Y. Assessing the impacts of climate change and habitat suitability on the distribution and quality of medicinal plant using multiple information integration: take *Gentiana rigescens* as an example. Ecol Indic. 2021;123:107376. https://doi.org/10.1016/j.ecolind.2021.107376.
68. Zhan X, Chen Z, Chen R, Shen C. Environmental and genetic factors involved in plant protection-associated secondary metabolite biosynthesis pathways. Front Plant Sci. 2022;13:1–14.
69. Li Y, Kong D, Fu Y, Sussman MR, Wu H. The effect of developmental and environmental factors on secondary metabolites in medicinal plants. Plant Physiol Biochem. 2020;148:80–9. https://doi.org/10.1016/j.plaphy.2020.01.006.
70. Yang M, Li Z, Liu L, Bo A, Zhang C, Li M. Ecological niche modeling of astragalus Membranaceus var. Mongholicus medicinal plants in inner Mongolia, China. Sci Rep. 2020;10:12482. https://doi.org/10.1038/s41598-020-69391-3.

Publisher's Note